

# CONSERVATION, CONVERGENCE, AND COMPUTATION FOR EVOLVING HETEROGENEOUS ELASTIC WIRES

ANNA DALL'ACQUA, GASPARD JANKOWIAK, LEONIE LANGER, AND FABIAN RUPP

**ABSTRACT.** The elastic energy of a bending-resistant interface depends both on its geometry and its material composition. We consider such a heterogeneous interface in the plane, modeled by a curve equipped with an additional density function. The resulting energy captures the complex interplay between curvature and density effects, resembling the Canham–Helfrich functional. We describe the curve by its inclination angle, so that the equilibrium equations reduce to an elliptic system of second order. After a brief variational discussion, we investigate the associated nonlocal  $L^2$ -gradient flow evolution, a coupled quasilinear parabolic problem. We analyze the (non)preservation of quantities such as convexity, positivity, and symmetry, as well as the asymptotic behavior of the system. The results are illustrated by numerical experiments.

**Keywords:** Euler–Bernoulli elastic energy, heterogeneous material, elastic flow, maximum principle, convexity, symmetry, asymptotic behavior.

**MSC(2020):** 35K40 (primary), 35Q92, 35B40, 35B06 (secondary).

## 1. INTRODUCTION

In shape optimization, the energy and thus the equilibrium configuration of a bending-resistant surface can depend both on its geometry as well as the distribution of some physical densities, representing, for example mass, electrostatic charge, temperature, etc. For instance, the shape can depend on the material composition and vice versa, as it is the case for certain biomembranes [23, 4, 31]. This phenomenon is not accounted for in the classical Canham–Helfrich model describing the characteristic biconcave shape of red blood cells [8, 20]. If the densities are discrete, a variational existence theory has been established, relying on either rotational symmetry [9, 22] or weak formulations using curvature varifolds [7].

A one-dimensional model which attributes for the aforementioned interplay between curvature and density-related effects has been introduced in [6], where closed planar curves are equipped with a (nondiscrete) density function. For the discrete setting, we refer to [21] and also mention a related discrete-to-continuum  $\Gamma$ -limit result [15]. Inspired by the Canham–Helfrich model depending on a spontaneous curvature, we define a generalized Euler–Bernoulli energy for a planar heterogeneous elastic wire  $\gamma$  with density function  $\rho$  by

$$(1.1) \quad \mathcal{E}_\mu(\gamma, \rho) = \frac{1}{2} \int_\gamma (\beta(\rho)(\kappa - c_0)^2 + \mu(\partial_s \rho)^2) \, ds.$$

Here,  $\beta$  is a smooth positive function, describing the density-modulated bending stiffness of the wire, the parameter  $c_0 \in \mathbb{R}$  denotes the spontaneous curvature, and  $\mu > 0$  models the diffusivity of the density. Further,  $\kappa$  is the signed curvature of  $\gamma$ ,  $ds = |\partial_x \gamma(x)| \, dx$  is the arc-length element, and  $\partial_s = |\partial_x \gamma(x)|^{-1} \partial_x$ . Consequently, the curve strives for a preferred curvature  $c_0 \in \mathbb{R}$  (determined by the material, see [31]), and the defect is penalized depending on the continuous density distribution. In the special case where  $\rho$  is constant and  $c_0 = 0$ , we essentially retrieve

the classical Euler–Bernoulli elastic energy given by

$$(1.2) \quad \mathcal{E}(\gamma) = \frac{1}{2} \int_{\gamma} \kappa^2 \, ds.$$

Critical points of (1.2) with prescribed length are called elasticae and have been classified in several previous works. In particular, the only closed elasticae are multifold coverings of the circle and of the figure eight elastica (depicted in Figure 12), see for instance [24], [14], or [33, Lemma 5.4]. Such a classification is, of course, not available for (1.1), but, as we shall see, elasticae play an important role also in this general case.

Actually, for planar curves, the order of the energy (1.1) may be reduced as follows. Since (1.1) is invariant under orientation preserving reparametrisations, we assume that the planar curve  $\gamma$  with prescribed length  $L$  is parametrized by arc-length. Then there exists an (inclination) angle function  $\theta: [0, L] \rightarrow \mathbb{R}$  such that  $\partial_s \gamma = (\cos \theta, \sin \theta)$ . Modulo isometries of  $\mathbb{R}^2$ , the curve  $\gamma$  together with its orientation is uniquely determined by  $\theta$ . More precisely, for some  $\gamma(0) \in \mathbb{R}^2$  we have

$$(1.3) \quad \gamma: [0, L] \rightarrow \mathbb{R}^2, \quad \gamma(s) = \int_0^s \begin{pmatrix} \cos \theta \\ \sin \theta \end{pmatrix} \, dr + \gamma(0).$$

With  $\theta$  and the density function  $\rho: [0, L] \rightarrow \mathbb{R}$ , the energy (1.1) can be expressed by

$$(1.4) \quad \mathcal{E}_{\mu}(\theta, \rho) = \frac{1}{2} \int_0^L (\beta(\rho)(\partial_s \theta - c_0)^2 + \mu(\partial_s \rho)^2) \, ds,$$

using that  $\kappa = \partial_s \theta$ , so that  $\mathcal{E}_{\mu}(\gamma, \rho) = \mathcal{E}_{\mu}(\theta, \rho)$ . Naturally, to achieve compactness, the variational discussion of (1.4) involves prescribing the length  $L$  and the rotation index  $\omega$  of the curve, and the integral of the density, i.e.

$$(1.5) \quad \int_0^L \rho \, ds = \nu L.$$

The length constraint and the preferred curvature  $c_0 \in \mathbb{R}$  are competing forces for minimizing  $\mathcal{E}_{\mu}$ , in general, since prescribing the length may not allow for a curve with constant curvature  $\kappa \equiv c_0$ . In the sequel, the constants  $L > 0$ ,  $\nu \in \mathbb{R}$ ,  $\mu > 0$ ,  $\omega \in \mathbb{Z}$ , and  $c_0 \in \mathbb{R}$ , are fixed, and we will refer to them as model parameters. For the bending stiffness  $\beta$ , we assume  $\beta \in C^{\infty}(\mathbb{R})$  and  $\beta > 0$ .

**1.1. Previous work.** The constrained minimization problem  $\min \mathcal{E}_{\mu}(\theta, \rho)$  with zero spontaneous curvature and rotation index equal to one was studied in [6]. In [10], some of the authors followed a dynamic approach and introduced the constrained  $L^2$ -gradient flow associated to (1.4). It can be used to describe, in the simplified quasistatic and viscous regime, the continuous deformation towards an energetically more favourable state. In addition to the constraints on length, rotation index, and the integral of the density, we need to ensure that the angle function describes a closed curve. Overall, this results in the initial boundary value problem

$$(1.6) \quad \begin{cases} \partial_t \theta = \partial_s (\beta(\rho)(\partial_s \theta - c_0)) + \lambda_{\theta 1} \sin \theta - \lambda_{\theta 2} \cos \theta & \text{in } (0, T) \times [0, L], \\ \partial_t \rho = \mu \partial_s^2 \rho - \frac{1}{2} \beta'(\rho)(\partial_s \theta - c_0)^2 - \lambda_{\rho} & \text{in } (0, T) \times [0, L], \\ \theta(\cdot, L) - \theta(\cdot, 0) = 2\pi\omega, \quad \rho(\cdot, L) = \rho(\cdot, 0) & \text{on } [0, T], \\ \partial_s \theta(\cdot, L) = \partial_s \theta(\cdot, 0), \quad \partial_s \rho(\cdot, L) = \partial_s \rho(\cdot, 0) & \text{on } [0, T], \\ \theta(0, \cdot) = \theta_0, \quad \rho(0, \cdot) = \rho_0 & \text{on } [0, L], \end{cases}$$

with  $(\theta_0, \rho_0) \in C^1([0, L])$  satisfying the boundary conditions. Since an angle function  $\theta: [0, L] \rightarrow \mathbb{R}$  represents a zeroth order closed curve if and only if

$$(1.7) \quad \int_0^L \sin \theta \, ds = \int_0^L \cos \theta \, ds = 0,$$

it is required that  $\theta_0$  satisfies (1.7). To ensure (1.7) along the flow, the nonlocal Lagrange multipliers  $\lambda_{\theta 1}$  and  $\lambda_{\theta 2}$  are given by

$$(1.8) \quad \begin{pmatrix} \lambda_{\theta 1}(t) \\ \lambda_{\theta 2}(t) \end{pmatrix} := \Pi^{-1}(\theta) \int_0^L \begin{pmatrix} \cos \theta \\ \sin \theta \end{pmatrix} \partial_s \theta \beta(\rho) (\partial_s \theta - c_0) \, ds,$$

where  $\Pi^{-1}(\theta)(t)$  denotes the inverse of the matrix

$$\Pi(\theta)(t) := \begin{pmatrix} \int_0^L \sin^2 \theta \, ds & - \int_0^L \cos \theta \sin \theta \, ds \\ - \int_0^L \cos \theta \sin \theta \, ds & \int_0^L \cos^2 \theta \, ds \end{pmatrix}.$$

The matrix  $\Pi$  is invertible as long as the angle function  $\theta$  describes a closed curve, see [10, Remark 2.1]. Moreover, the nonlocal Lagrange multiplier  $\lambda_\rho$  is chosen as

$$(1.9) \quad \lambda_\rho(t) := -\frac{1}{2L} \int_0^L \beta'(\rho) (\partial_s \theta - c_0)^2 \, ds.$$

This ensures conservation of the total mass, i.e. (1.5) is preserved along the evolution. For the convenience of the reader, we recall the previous results on existence and convergence which we build upon, see [10, Theorems 1.2–1.4, Lemma 3.5, and Remark 3.7].

**Theorem 1.1.** *Suppose the initial datum  $(\theta_0, \rho_0) \in C^\infty([0, L])$  satisfies (1.5), (1.7), and*

$$\begin{aligned} \theta_0(L) - \theta_0(0) &= 2\pi\omega, & \partial_s \theta_0(L) &= \partial_s \theta_0(0), & \partial_s^2 \theta_0(L) &= \partial_s^2 \theta_0(0), \\ \rho_0(L) &= \rho_0(0), & \partial_s \rho_0(L) &= \partial_s \rho_0(0), & \partial_s^2 \rho_0(L) &= \partial_s^2 \rho_0(0). \end{aligned}$$

*Then, there exists a unique global solution  $(\theta, \rho) \in C^\infty((0, \infty) \times [0, L]) \cap C^0([0, \infty); C^2([0, L]))$  of (1.6), depending continuously on the initial datum  $(\theta_0, \rho_0)$ . For all  $t > 0$ ,  $\kappa(t, \cdot) = \partial_s \theta(t, \cdot)$  and  $\rho(t, \cdot)$  can be extended to smooth  $L$ -periodic functions on  $\mathbb{R}$ . Moreover, the solution satisfies*

$$\limsup_{t \rightarrow \infty} (\|\theta(t)\|_{W^{3,2}(0,L)} + \|\rho(t)\|_{W^{3,2}(0,L)}) < \infty,$$

*and subconverges, as  $t \rightarrow \infty$ , in  $C^2([0, L])$  to a stationary solution, i.e. a solution of*

$$(1.10) \quad \begin{cases} 0 = \partial_s (\beta(\rho) (\partial_s \theta - c_0)) + \lambda_{\theta 1} \sin \theta - \lambda_{\theta 2} \cos \theta & \text{in } [0, L], \\ 0 = \mu \partial_s^2 \rho - \frac{1}{2} \beta'(\rho) (\partial_s \theta - c_0)^2 - \lambda_\rho & \text{in } [0, L], \\ \theta(L) - \theta(0) = 2\pi\omega, \quad \rho(L) = \rho(0), \\ \partial_s \theta(L) = \partial_s \theta(0), \quad \partial_s \rho(L) = \partial_s \rho(0), \\ \partial_s^2 \theta(L) = \partial_s^2 \theta(0), \quad \partial_s^2 \rho(L) = \partial_s^2 \rho(0) \end{cases}$$

*for some  $\lambda_{\theta 1}, \lambda_{\theta 2}, \lambda_\rho \in \mathbb{R}$ . If, in addition,  $\beta$  is real analytic, then we have full convergence  $(\theta(t), \rho(t)) \rightarrow (\theta_\infty, \rho_\infty)$  in  $C^2([0, L])$  as  $t \rightarrow \infty$ , for some  $(\theta_\infty, \rho_\infty)$  solving (1.10).*

We will refer to a smooth function  $(\theta_0, \rho_0)$  satisfying the assumptions of Theorem 1.1 as an *admissible initial datum* in the sequel.

The global existence and convergence of the system (1.6) is in accordance with previous work on the elastic flow, i.e. the  $L^2$ -gradient flow of (1.2), both in its fourth order version for curves [16, 30, 25, 11, 13, 12, 29, 34] and its second order flow for the angle function in the planar case [38, 35, 26, 36]. Due to a lack of maximum principle, along the fourth order flow properties like convexity or embeddedness of the initial datum do not need to be preserved [5, 32], see also [27].

As we shall see, for the second order system (1.6) such properties depend delicately on the choice of the model parameters.

Lastly, we mention that a similar system relating mean curvature flow and diffusion of a density on a hypersurface has been studied in [2, 1].

**1.2. Main results and structure of the article.** This article extends the results obtained in [10] and investigates several properties of solutions to (1.6), a quasilinear coupled parabolic system of second order involving nonlocal Lagrange multipliers.

Our work is inspired by the analysis of preserved quantities for curvature flows of hypersurfaces by Escher–Ito [18] and by Wen’s article [38] on the gradient flow of (1.2) in terms of  $\theta$ . We focus mainly on two aspects: the (non)preservation of several properties of the initial datum along the evolution and the discussion of conditions under which the limit and the rate of convergence of the system can be determined. Since the limit configuration is a constrained critical point of (1.4), this also provides a partial classification of constrained critical points of  $\mathcal{E}_\mu$ . We complement the analysis by numerical experiments that have motivated our results.

In Section 2, as a first step towards understanding the asymptotic behavior, we examine minimizers and constrained critical points of the functional, which are precisely the stationary solutions. As indicated by the form of the energy (1.4), a global minimizer has to have constant density if  $\mu$  is sufficiently large, cf. also [6] for the case  $\omega = 1$ ,  $c_0 = 0$ . Remarkably, this is generically not true on the level of critical points, see Example 2.13. We provide sharp sufficient conditions for constrained critical points to be homogeneous elasticae, i.e. elasticae with constant density.

In Section 3, we study the (non)preservation of properties of the initial datum along (1.6). The decisive advantage of working with the angle function  $\theta$  is that the equation is of second order. In contrast, working with the curve  $\gamma$  yields a fourth order equation, like the classical elastic flow. Due to the reduction to second order, parabolic maximum principles are available for both evolution equations in (1.6) individually, but of course not for the full system. A key difficulty in applying maximum principles is the structure of the relevant evolution equations, explaining the fundamentally different behavior for  $c_0 = 0$  compared to  $c_0 \neq 0$ .

First, we adapt the methods in [3] to study the inflection points of the curve, i.e. the sign changes of the curvature.

**Theorem 1.2.** *Let  $c_0 = 0$  and let  $(\theta, \rho)$  be a global solution of (1.6). Then both the number of zeros of  $\kappa = \partial_s \theta$  and the number of inflection points of the associated curve are nonincreasing in time.*

Combining this result with further maximum principle arguments, we examine (strict) convexity along the evolution.

**Theorem 1.3** (Preservation of convexity for  $c_0 = 0$ ). *Let  $(\theta, \rho)$  be the global solution of (1.6) with admissible initial datum  $(\theta_0, \rho_0)$  and  $c_0 = 0$ . Then*

- (i)  $\kappa_0 \geq 0$  ( $\kappa_0 \leq 0$ ) on  $[0, L]$  implies  $\kappa \geq 0$  ( $\kappa \leq 0$ ) on  $[0, \infty) \times [0, L]$ ;
- (ii)  $\kappa_0 > 0$  ( $\kappa_0 < 0$ ) on  $[0, L]$  implies  $\kappa > 0$  ( $\kappa < 0$ ) on  $[0, \infty) \times [0, L]$ .

Both Theorem 1.2 and Theorem 1.3 rely heavily on the vanishing of  $c_0$ . Indeed, even for  $|c_0| \neq 0$  small, convexity is not preserved in general (see Example 3.7). This behavior is not easily predicted from the energy, since e.g. a large positive  $c_0$  clearly favors positive curvature. Moreover, despite the nonlinear structure of the equation for the density, under appropriate sharp assumptions on  $\beta$  we are still able to apply maximum principles to examine sign-preservation of the density, see Proposition 3.8.

For the curve shortening flow, a classical application of the maximum principle is the preservation of embeddedness, cf. [19]. While the evolution of the curves obtained via (1.3) does not allow

for these methods, we are still able to find an embeddedness-preserving energy threshold in Proposition 3.11.

Further, we show in Section 3.6 that both  $k$ -fold rotational symmetry and axial symmetry of the initial datum are preserved along the evolution (see Propositions 3.15 and 3.19), for simplicity restricting to the case  $\omega = 1$ . In the rotationally symmetric case, the Lagrange multipliers  $\lambda_{\theta 1}$  and  $\lambda_{\theta 2}$  vanish, which enables us to generalize Theorem 1.3 for a  $k$ -fold rotationally symmetric initial datum as follows.

**Theorem 1.4.** *Let  $\omega = 1$ ,  $k \geq 2$  and  $c_0 \in \mathbb{R}$ . Let  $(\theta_0, \rho_0)$  be an admissible initial datum corresponding to a  $k$ -fold rotationally symmetric heterogeneous curve with  $\kappa_0 \geq c_0$  on  $[0, L]$  and let  $(\theta, \rho)$  be the solution of (1.6). Then  $\kappa \geq c_0$  on  $[0, \infty) \times [0, L]$ . Similarly, if  $\kappa_0 \leq c_0$  on  $[0, L]$ , then  $\kappa \leq c_0$  on  $[0, \infty) \times [0, L]$ .*

The convergence result in [10] naturally raises the question of a characterization of the limit, which we can answer despite the large number of selectable parameters under suitable assumptions on  $\beta$ ,  $\nu$ , and  $\mu$  in Section 4. To that end, we rely on the properties of constrained critical points that we discussed in Section 2.

**Theorem 1.5** (Asymptotic behavior under growth assumptions on  $\beta$ ). *Suppose there exists  $\bar{C} \geq 0$  such that*

$$(1.11) \quad \beta'(x)(\nu - x) \leq \bar{C}\beta(x)(\nu - x)^2 \quad \text{for all } x \in \mathbb{R}.$$

*Let  $(\theta_0, \rho_0)$  be an admissible initial datum with  $\bar{C}L\mathcal{E}_\mu(\theta_0, \rho_0) < \mu$ . Then the density  $\rho$  of the solution  $(\theta, \rho)$  to (1.6) converges exponentially fast to  $\rho_\infty \equiv \nu$  in  $C^2([0, L])$  as  $t \rightarrow \infty$ . Moreover,*

- (i) *if  $\omega \neq 0$ , then  $\theta(t) \rightarrow \theta_\infty$  in  $C^2([0, L])$ , where  $\theta_\infty$  describes a  $\omega$ -fold covered circle;*
- (ii) *if  $\omega = 0$  and  $\beta$  is analytic, then  $\theta(t) \rightarrow \theta_\infty$  in  $C^2([0, L])$ , where  $\theta_\infty$  describes a multifold covered figure eight elastica.*

Assumption (1.11) is clearly satisfied if we have  $\beta'(\nu) = 0$ ,  $\|\beta''\|_\infty < \infty$ , and  $\inf_{\mathbb{R}} \beta > 0$ . If  $\beta$  is such that  $\beta'(x)(\nu - x) \leq 0$  for  $x \in \mathbb{R}$ , we may choose  $\bar{C} = 0$  in (1.11). In this case, there is no assumption on the initial energy. We highlight that, remarkably, analyticity is not needed for the case  $\omega \neq 0$ , see the discussion after the proof of Theorem 1.5 in Section 4.1.

For rotationally symmetric initial data ( $\omega = 1$ ) and  $c_0 = \frac{2\pi}{L}$  we prove exponential convergence to a circle with constant density without further assumptions, see Proposition 4.1. Furthermore, we can determine the limit for large values of  $\mu$  and constant initial density.

**Theorem 1.6** (Asymptotic behavior for large  $\mu$ ). *Let  $\omega \neq 0$  and suppose that  $\beta$  is real analytic. Let  $(\theta_0, \rho_0)$  be an admissible initial datum with  $\rho_0 \equiv \nu$ . There exists  $\mu_0 \in (0, \infty)$  such that if  $\mu \geq \mu_0$ , then the limit  $(\theta_\infty, \rho_\infty)$  of Theorem 1.1 describes an  $\omega$ -fold covered circle with constant density.*

A major difficulty here is that the two parts of the energy do not decrease individually, so that the density does not remain constant, in general.

In Section 5, we propose a simple numerical scheme approximating solutions to (1.6) which takes advantage of the gradient flow structure of the problem and is based on De Giorgi's Minimizing Movements and finite differences, extending the idea of [6] to the more general and time-dependent system. Our analysis is substantially guided by the resulting computations, especially concerning the long-term behavior of the system. Numerical experiments allow us to explore qualitative properties of the flow beyond the scope covered in the previous sections. We consider a number of examples, some of which are: the loss of embeddedness in two cases, first in the case of some  $c_0 > 2\pi/L$ , and second in the more subtle case of  $c_0 = 0$ , with a careful choice of the initial data; the convergence to nontrivial states for  $\mu$  small, which hints at the existence of

nontrivial critical points, even for rotationally symmetric initial data; the impact of the choice of parameters on the limit configuration  $(\theta_\infty, \rho_\infty)$ ; and finally the instability of multiple coverings of the figure eight, in the case  $\omega = 0$ .

For a related problem on surfaces, we would like to point out that two finite element methods are proposed and analyzed in [17], based on a more geometric approach.

## 2. THE STATIC PROBLEM

**2.1. The Euler–Lagrange equations.** For  $k \in \mathbb{N}$ , we denote the Hilbert space of periodic Sobolev functions on  $[0, L]$  by

$$W_{\text{per}}^{k,2}(0, L) := \{u \in W^{k,2}(0, L) : \partial_s^\ell u(L) = \partial_s^\ell u(0) \text{ for } \ell = 0, \dots, k-1\}.$$

The standard angle function of an  $\omega$ -fold covering of the circle is given by

$$(2.1) \quad \phi(s) = \frac{2\pi\omega s}{L} \quad \text{for } s \in [0, L],$$

see [10, Section 3.1]. If  $\theta \in W^{k,2}(0, L)$  is an angle function for a  $C^k$ -closed curve with rotation index  $\omega \in \mathbb{Z}$ , there exists a unique  $u \in W_{\text{per}}^{k,2}(0, L)$  such that  $\theta = \phi + u$ . Consequently, it is natural to study the energy  $\mathcal{E}_\mu$  defined in (1.4) on the set

$$\mathcal{U} := W_{\text{per}}^{1,2}(0, L; \mathbb{R}^2) + (\phi, 0) = \{(\theta, \rho) \in W^{1,2}(0, L; \mathbb{R}^2) : \theta(L) - \theta(0) = 2\pi\omega, \rho(L) = \rho(0)\}.$$

By introducing the constraint functional

$$\mathcal{G}(\theta, \rho) = \left( \int_0^L \cos \theta \, ds, \int_0^L \sin \theta \, ds, \int_0^L \rho \, ds - \nu L \right),$$

we see that  $(\theta, \rho) \in \mathcal{U}$  corresponds to a  $C^1$ -closed curve with rotation index  $\omega \in \mathbb{Z}$  and a density with total mass  $\nu L$  if and only if  $\mathcal{G}(\theta, \rho) = 0$ . We thus define the side condition  $\mathcal{A} := \{(\theta, \rho) \in \mathcal{U} : \mathcal{G}(\theta, \rho) = 0\}$ . The set  $\mathcal{U}$  is not a vector space (unless  $\omega = 0$ ), but only an affine subspace of the Hilbert space  $W^{1,2}(0, L; \mathbb{R}^2)$ . However, this causes only some minor technical difficulties which can be resolved by working in the periodic setting with the shifted functionals

$$\begin{aligned} E_\mu : W_{\text{per}}^{1,2}(0, L; \mathbb{R}^2) &\rightarrow \mathbb{R}, \quad E_\mu(u, \rho) = \mathcal{E}_\mu(u + \phi, \rho), \\ G : W_{\text{per}}^{1,2}(0, L; \mathbb{R}^2) &\rightarrow \mathbb{R}^3, \quad G(u, \rho) = \mathcal{G}(u + \phi, \rho), \end{aligned}$$

with  $\phi$  as in (2.1).

It can be checked that  $\mathcal{G}'(\theta, \rho) : W_{\text{per}}^{1,2}(0, L; \mathbb{R}^2) \rightarrow \mathbb{R}^3$ , for  $(\theta, \rho) \in \mathcal{A}$ , is surjective. Hence, applying [39, Proposition 43.21], we see that the energy  $\mathcal{E}_\mu$  has a critical point subject to the constraint  $\mathcal{G} = 0$  at some  $(\theta, \rho) \in \mathcal{A}$  if and only if there exist  $\lambda_{\theta 1}, \lambda_{\theta 2}, \lambda_\rho \in \mathbb{R}$  such that

$$(2.2) \quad 0 = \int_0^L (\beta(\rho)(\partial_s \theta - c_0) \partial_s v - \lambda_{\theta 1} \sin \theta v + \lambda_{\theta 2} \cos \theta v) \, ds,$$

$$(2.3) \quad 0 = \int_0^L (\mu \partial_s \rho \partial_s \sigma + \frac{1}{2} \beta'(\rho)(\partial_s \theta - c_0)^2 \sigma + \lambda_\rho \sigma) \, ds$$

for all  $(v, \sigma) \in W_{\text{per}}^{1,2}(0, L; \mathbb{R}^2)$ . Choosing appropriate test functions shows that  $\lambda_{\theta 1}, \lambda_{\theta 2}$  and  $\lambda_\rho$  are given as in (1.8), and (1.9). If the constrained critical point  $(\theta, \rho)$  is more regular, precisely  $(\theta, \rho) \in W_{\text{per}}^{2,2}(0, L; \mathbb{R}^2) + (\phi, 0)$ , (2.2) and (2.3) yield the *Euler–Lagrange equations*

$$(2.4) \quad 0 = \partial_s (\beta(\rho)(\partial_s \theta - c_0)) + \lambda_{\theta 1} \sin \theta - \lambda_{\theta 2} \cos \theta,$$

$$(2.5) \quad 0 = \mu \partial_s^2 \rho - \frac{1}{2} \beta'(\rho)(\partial_s \theta - c_0)^2 - \lambda_\rho.$$

**2.2. Existence of minimizers and smoothness of critical points.** The existence of a solution to the minimization problem

$$(2.6) \quad \inf_{(\theta, \rho) \in \mathcal{A}} \mathcal{E}_\mu(\theta, \rho) \longrightarrow \min!$$

can be shown via the direct method following the arguments in [6, Prop. 3.2], also in the case of general winding number  $\omega \in \mathbb{Z}$ , and with spontaneous curvature  $c_0 \in \mathbb{R}$ .

**Proposition 2.1** (Existence of a minimizer). *There exists  $(\theta^*, \rho^*) \in \mathcal{A}$  such that  $\mathcal{E}_\mu(\theta^*, \rho^*) = \inf_{(\theta, \rho) \in \mathcal{A}} \mathcal{E}_\mu(\theta, \rho)$ .*

We prove now that constrained critical points (and in particular minimizers) are smooth.

**Proposition 2.2** (Smoothness of critical points). *If  $(\theta, \rho)$  is a constrained critical point, the  $L$ -periodic extension of  $(\partial_s \theta, \partial_s \rho)$  to  $\mathbb{R}$  is smooth. In particular,  $(\theta, \rho) \in C^\infty([0, L])$  and  $\partial_s \theta(L) = \partial_s \theta(0)$ ,  $\partial_s \rho(L) = \partial_s \rho(0)$ .*

*Proof.* Let  $(\theta, \rho) \in \mathcal{U}$  be a constrained critical point. Then there exist  $\lambda_{\theta 1}, \lambda_{\theta 2}, \lambda_\rho \in \mathbb{R}$  such that  $(\theta, \rho)$  satisfies (2.2) and (2.3).

*Step 1:*  $(\theta, \rho) \in W^{2,2}(0, L) \subset C^1([0, L])$ . Since  $\rho \in W^{1,2}(0, L) \subset C([0, L])$ ,  $\|\beta' \circ \rho\|_{C([0, L])}$  and  $\|\partial_s \rho\|_{L^2(0, L)}$  are bounded. Thus, (2.2) implies that there is  $C = C(\theta, \rho)$  such that

$$\left| \int_0^L \beta(\rho) \partial_s \theta \partial_s v \, ds \right| = \left| \int_0^L (\lambda_{\theta 1} \sin \theta - \lambda_{\theta 2} \cos \theta) v \, ds - \int_0^L \beta'(\rho) \partial_s \rho c_0 v \, ds \right| \leq C \|v\|_{L^2(0, L)}$$

for all  $v \in C_c^1((0, L)) \subset W_{\text{per}}^{1,2}(0, L)$ . So,  $\beta(\rho) \partial_s \theta \in W^{1,2}(0, L)$ . Hence,  $\|\beta(\rho)(\partial_s \theta - c_0)\|_{C([0, L])}$  and also  $\|\beta'(\rho)(\partial_s \theta - c_0)\|_{C([0, L])}$  are bounded, so (2.3) implies that

$$2\mu \left| \int_0^L \partial_s \rho \partial_s \sigma \, ds \right| = \left| \int_0^L (-\beta'(\rho)(\partial_s \theta - c_0)^2 \sigma - 2\lambda_\rho \sigma) \, ds \right| \leq C \|\sigma\|_{L^2(0, L)}$$

for all  $\sigma \in C_c^1((0, L))$ . It follows that  $\rho \in W^{2,2}(0, L) \subset C^1([0, L])$ . We thus obtain  $\partial_s(\beta(\rho) \partial_s \theta) = \beta'(\rho) \partial_s \rho \partial_s \theta + \beta(\rho) \partial_s^2 \theta$  in the sense of distributions, so  $\partial_s^2 \theta \in L^2(0, L)$  as  $\inf_{[0, L]} \beta(\rho) > 0$ .

*Step 2:*  $(\theta, \rho) \in W^{3,2}(0, L) \subset C^2([0, L])$ . The increased regularity yields that  $(\theta, \rho)$  satisfies (2.4) and (2.5) in  $L^2(0, L)$ . Using the same ideas as in Step 1, we can deduce that  $(\theta, \rho) \in W^{3,2}(0, L)$ .

*Step 3: Smooth  $L$ -periodic extension.* Testing (2.2) and (2.3) with  $W_{\text{per}}^{1,2}$ -functions not vanishing at the boundary results in the natural boundary conditions

$$(2.7) \quad \partial_s \theta|_0^L = 0 \quad \text{and} \quad \partial_s \rho|_0^L = 0.$$

Since  $(\theta, \rho)$  satisfies (2.4) and (2.5) pointwise we conclude with (2.7) that  $\partial_s^2 \theta(L) = \partial_s^2 \theta(0)$  and  $\partial_s^2 \rho(L) = \partial_s^2 \rho(0)$ . The claim follows by bootstrapping.  $\square$

**2.3. Homogeneous elastica.** The structure of the energy functional  $\mathcal{E}_\mu$  suggests that for large values of  $\mu$ , minimizers favor almost constant density, cf. [6]. For constant density,  $\mathcal{E}_\mu$  is essentially the elastic energy whose critical points are called elasticae. For  $\mu$  large, these elasticae also play an important role for the heterogeneous elastic energy (1.4).

**Definition 2.3.** Let  $(\theta, \rho) \in \mathcal{A}$ . We say that  $\theta$  describes a *(length-constrained) elastica* if the curvature  $\kappa = \partial_s \theta$  is smooth and satisfies the *constrained elastica equation*

$$(2.8) \quad \partial_s^2 \kappa + \frac{1}{2} \kappa^3 - \lambda \kappa = 0 \quad \text{for some } \lambda \in \mathbb{R}.$$

If further  $\rho$  is constant, we say that  $(\theta, \rho)$  describes a *homogeneous elastica*.

Solutions of (2.8) have been classified explicitly in several previous works, see for example [24], [14], or [33, Lemma 5.4]. In the case of closed curves, the elasticae can be characterized as follows.

**Lemma 2.4** ([24]). *The only closed constrained elasticae are multifold coverings of circles and multifold coverings of the figure eight (elastica).*

The figure eight is illustrated in Figure 12 on page 32.

**Remark 2.5.** Let  $(\theta, \rho) \in \mathcal{A}$ . If  $\omega \neq 0$  and  $\theta$  describes an elastica, then  $\theta$  is the angle function of an  $\omega$ -fold covering of a circle with curvature  $\kappa = \frac{2\pi\omega}{L}$ . Thus,  $\theta$  is determined up to an additive constant. If  $(\theta, \rho)$  describes a homogeneous elastica and we require that  $\theta(0) = 0$  or that  $\int_0^L \theta(s) ds = \pi\omega L$ , then

$$(\theta, \rho) = (\theta_c, \rho_c) := \left( \frac{2\pi\omega}{L} s, \nu \right) \in \mathcal{A}.$$

2.3.1. *Minimizers and critical points for large  $\mu$ .* We now show that for large values of  $\mu$  and  $\omega \neq 0$ , a minimizer  $(\theta, \rho)$  in (2.6) describes a homogeneous elastica. To state a uniqueness result, we define  $\mathcal{I}(\theta) := \int_0^L \theta(s) ds$  and fix  $\mathcal{I}(\theta) = \pi\omega L$ .

**Proposition 2.6** (Unique minimizer for large  $\mu$ ). *Let  $\omega \neq 0$ . Then there exists  $\mu_0 \in (0, \infty)$  such that if  $\mu \geq \mu_0$ ,  $\mathcal{E}_\mu(\theta_c, \rho_c) < \mathcal{E}_\mu(\theta, \rho)$  for all  $(\theta, \rho) \in \mathcal{A} \cap \{\mathcal{I}(\theta) = \pi\omega L\} \setminus \{(\theta_c, \rho_c)\}$ .*

The proof can essentially be done as in [6, Prop. 3.3] which is why we only outline the idea here.

*Idea of the proof.* In a first step, one shows that for  $\mu$  large enough, the second variation  $\mathcal{E}_\mu''(\theta_c, \rho_c)$  is strictly positive. It follows (for example with [39, Theorem 43.D]) that  $(\theta_c, \rho_c)$  is a strict local minimizer in the sense that there exists  $\delta = \delta(\mu) > 0$  such that  $\mathcal{E}_\mu(\theta_c, \rho_c) < \mathcal{E}_\mu(\theta, \rho)$  for all  $(\theta, \rho) \in \mathcal{A} \cap \{\mathcal{I}(\theta) = \pi\omega L\} \setminus \{(\theta_c, \rho_c)\}$  with norm  $\|(\theta, \rho) - (\theta_c, \rho_c)\|_{W^{1,2}(0,L)} < \delta$ . Now, note that  $\mathcal{E}_\mu(\theta_c, \rho_c)$  is independent of  $\mu$  whereas  $\mathcal{E}_\mu(\theta, \rho)$  is increasing in  $\mu$ . Consequently, the neighborhood in which  $(\theta_c, \rho_c)$  is a strict local minimizer can be chosen only depending on a lower bound  $\mu_1$  on  $\mu$ . In a second step, one proves that there exists  $\mu_2$  such that for  $\mu > \mu_2$ , all global minimizers are contained in  $B_\delta(\theta_c, \rho_c) \subset W^{1,2}(0, L)$ . Together with the first step, for  $\mu > \max\{\mu_1, \mu_2\}$ ,  $(\theta_c, \rho_c)$  is the unique global minimizer with  $\mathcal{I}(\theta) = \pi\omega L$ .  $\square$

This result does not extend to  $\omega = 0$ , see Remark 2.10. The next example shows that  $(\theta_c, \rho_c)$  does not always need to be a global minimizer.

**Example 2.7.** Consider the double-well potential  $\beta(x) := (x^2 - 1)^2 + c$  with  $c > 0$ . Let  $L = 2\pi$ ,  $\omega = 1$ ,  $c_0 = 0$  and  $\nu = 0$ . Consider  $\theta_c = s$ ,  $\rho_c = 0$  and  $\rho := \sin(2s)$ . Then  $(\theta_c, \rho) \in \mathcal{A}$  and  $\mathcal{E}_\mu(\theta_c, \rho_c) = (1 + c)\pi > \left(\frac{3}{8} + c + \frac{\mu}{2}\right)\pi = \mathcal{E}_\mu(\theta_c, \rho)$  for  $\mu < \frac{5}{4}$ .

For large  $\mu$ ,  $(\theta_c, \rho_c)$  is also locally the unique constrained critical point. This follows from the continuity of  $\mathcal{E}_\mu''$  and  $\mathcal{G}''$  and the positive definiteness of  $\mathcal{E}_\mu''(\theta_c, \rho_c)$ .

**Corollary 2.8.** *Let  $\omega \neq 0$ . There is  $\mu_0 > 0$  and a  $C^1$ -neighborhood  $\mathcal{O}$  of  $(\theta_c, \rho_c)$  such that if  $(\theta, \rho) \in \mathcal{O}$  is a constrained critical point with  $\mathcal{I}(\theta) = \pi\omega L$  and  $\mu > \mu_0$ , then  $(\theta, \rho) = (\theta_c, \rho_c)$ .*

2.3.2. *Conditions for homogeneous elastica.* If a constrained critical point has constant density, this already implies that it describes a homogeneous elastica.

**Lemma 2.9.** *If  $(\theta, \rho)$  describes a constrained critical point and  $\rho \equiv \nu$ , then  $\theta$  describes an elastica.*

*Proof.* By Proposition 2.2,  $(\theta, \rho)$  is smooth. Since  $\rho$  is constant, the Euler–Lagrange equation (2.4) reads

$$(2.9) \quad 0 = \beta(\nu) \partial_s \kappa + \lambda_{\theta 1} \sin \theta - \lambda_{\theta 2} \cos \theta,$$

with  $\kappa = \partial_s \theta$ . As in [35, Remark 2.2], we multiply (2.9) with  $\kappa$ . This yields  $0 = \frac{1}{2} \beta(\nu) \partial_s(\kappa^2) + \partial_s(-\lambda_{\theta 1} \cos \theta - \lambda_{\theta 2} \sin \theta)$ . So there is  $\tilde{\lambda} \in \mathbb{R}$  such that

$$(2.10) \quad \tilde{\lambda} = \frac{1}{2} \beta(\nu) \kappa^2 - \lambda_{\theta 1} \cos \theta - \lambda_{\theta 2} \sin \theta.$$

Differentiation of (2.9) and inserting (2.10) leads to (2.8) with  $\lambda = \tilde{\lambda}/\beta(\nu)$ .  $\square$

**Remark 2.10.** In the case  $\omega = 0$ , a constrained critical point with constant density exists only if  $\beta'(\nu) = 0$ . Indeed, if  $\rho \equiv \nu$  and  $\beta'(\nu) \neq 0$ , it follows from (2.5) that  $(\partial_s \theta - c_0)^2$  is constant. For  $\omega = 0$ , this contradicts the closedness of the curve described by  $\theta$ .

For  $\omega \neq 0$  and under suitable assumptions on  $\beta$ , the converse implication of Lemma 2.9 also holds.

**Lemma 2.11.** *Let  $\omega \neq 0$  and  $c_0 \neq \frac{2\pi\omega}{L}$ . Let  $(\theta, \rho)$  be a constrained critical point and suppose  $\theta$  describes an elastica. If  $\beta$  is such that*

(a)  $\beta$  is convex or

$$(b) |\beta'(x)| < 2\mu \left( \frac{2\pi}{2\pi\omega - Lc_0} \right)^2 |\nu - x| \text{ or}$$

$$(c) \sup |\beta''| < 2\mu \left( \frac{2\pi}{2\pi\omega - Lc_0} \right)^2,$$

then  $\rho$  is constant. In particular,  $(\theta, \rho)$  describes a homogeneous elastica.

*Proof.* Since  $\theta$  describes a constrained closed elastica and  $\omega \neq 0$ , we have  $\kappa = \partial_s \theta \equiv \frac{2\pi\omega}{L}$  by Remark 2.5. The Euler–Lagrange equation for  $\rho$  (cf. (2.5)) simplifies to

$$(2.11) \quad \partial_s^2 \rho = \frac{(\kappa - c_0)^2}{2\mu} \left( \beta'(\rho) - \frac{1}{L} \int_0^L \beta'(\rho) \, ds \right).$$

(a) Using integration by parts,  $\int_0^L \rho \, ds = \nu L$ , and the convexity of  $\beta$ , we have

$$\int_0^L (\partial_s \rho)^2 \, ds = -\frac{(\kappa - c_0)^2}{2\mu} \int_0^L \beta'(\rho)(\rho - \nu) \, ds = -\frac{(\kappa - c_0)^2}{2\mu} \int_0^L (\beta'(\rho) - \beta'(\nu))(\rho - \nu) \, ds \leq 0.$$

(b) First, we proceed as in (a), then we obtain with  $(\kappa - c_0)^2 = \left( \frac{2\pi}{L} \right)^2 \left( \frac{2\pi\omega - Lc_0}{2\pi} \right)^2$ , the assumption on  $\beta'$ , and the Wirtinger inequality that

$$\int_0^L (\partial_s \rho)^2 \, ds = -\frac{(\kappa - c_0)^2}{2\mu} \int_0^L \beta'(\rho)(\rho - \nu) \, ds < \left( \frac{2\pi}{L} \right)^2 \int_0^L (\rho - \nu)^2 \, ds \leq \int_0^L (\partial_s \rho)^2 \, ds.$$

(c) We write  $\overline{\beta'(\rho)} = \frac{1}{L} \int_0^L \beta'(\rho) \, ds$  and use the Wirtinger inequality twice to get

$$\begin{aligned} \int_0^L (\partial_s^2 \rho)^2 \, ds &= \left( \frac{(\kappa - c_0)^2}{2\mu} \right)^2 \int_0^L (\beta'(\rho) - \overline{\beta'(\rho)})^2 \, ds \leq \frac{(\kappa - c_0)^4}{(2\mu)^2} \left( \frac{L}{2\pi} \right)^2 \int_0^L (\beta''(\rho) \partial_s \rho)^2 \, ds \\ &< \left( \frac{2\pi}{L} \right)^2 \int_0^L (\partial_s \rho)^2 \, ds \leq \int_0^L (\partial_s^2 \rho)^2 \, ds. \end{aligned}$$

In all cases, the periodic boundary conditions imply that  $\rho \equiv \nu$ .  $\square$

**Corollary 2.12** (of Theorem 1.5). *Let  $(\theta, \rho)$  be a constrained critical point. If  $\beta$  is such that  $\beta'(x) \leq 0$  for  $x < \nu$  and  $\beta'(x) \geq 0$  otherwise, then  $(\theta, \rho)$  describes a homogeneous elastica.*

Without additional assumptions on  $\beta$ , the density of a constrained critical point describing an elastica might be nonconstant.

**Example 2.13.** Let  $L = 2\pi$ ,  $\omega = 2$ ,  $\nu = 0$  and let  $\mu > 0$  and  $c_0 \neq 2$  be chosen such that  $(2 - c_0)^2 = 2\mu$ . Let  $\beta(x) = -\frac{x^2}{2} + 1$  for  $-1 \leq x \leq 1$ . Then both  $(\theta = \theta_c, \rho \equiv \nu) \in \mathcal{A}$  and  $(\theta = \theta_c, \rho = \sin s) \in \mathcal{A}$  are constrained critical points. In this case, inequalities (b) and (c) in Lemma 2.11 are attained with equality, so the assumptions are sharp.

**Remark 2.14.** For  $\omega \neq 0$ ,  $c_0 = \frac{2\pi\omega}{L}$  and  $(\theta, \rho)$  a constrained critical point with  $\theta$  describing an elastica, it follows directly from (2.11) and the periodic boundary conditions that  $\rho$  is constant.

### 3. QUALITATIVE PROPERTIES OF SOLUTIONS

**3.1. Decrease of the energy.** The  $L^2$ -gradient structure of the flow equations in (1.6) ensures that the energy  $\mathcal{E}_\mu$  decreases along the evolution. On the other hand, the two parts of the energy,

$$\mathcal{E}^\theta(\theta, \rho) := \frac{1}{2} \int_0^L \beta(\rho)(\partial_s \theta - c_0)^2 \, ds \quad \text{and} \quad \mathcal{E}_\mu^\rho(\rho) := \frac{\mu}{2} \int_0^L (\partial_s \rho)^2 \, ds$$

are not monotonically decreasing individually as the computation

$$\begin{aligned} \frac{d}{dt} \mathcal{E}_\mu(\theta, \rho) &= \int_0^L \left( \frac{1}{2} \beta'(\rho)(\partial_s \theta - c_0)^2 \partial_t \rho + \beta(\rho)(\partial_s \theta - c_0) \partial_t \partial_s \theta \right) \, ds + \int_0^L \mu \partial_s \rho \partial_s \partial_t \rho \, ds \\ &= - \int_0^L \partial_s (\beta(\rho)(\partial_s \theta - c_0)) \partial_t \theta \, ds + \int_0^L \left( \frac{1}{2} \beta'(\rho)(\partial_s \theta - c_0)^2 - \mu \partial_s^2 \rho \right) \partial_t \rho \, ds \\ &= - \int_0^L \partial_t \theta (\partial_t \theta - \lambda_{\theta 1} \sin \theta + \lambda_{\theta 2} \cos \theta) \, ds - \int_0^L \partial_t \rho (\partial_t \rho + \lambda_\rho) \, ds \\ (3.1) \quad &= - \int_0^L (\partial_t \theta)^2 \, ds - \int_0^L (\partial_t \rho)^2 \, ds \leq 0 \end{aligned}$$

already suggests. This fact significantly complicates the discussion of the limit in Section 4. We give concrete examples where either  $\mathcal{E}^\theta$  or  $\mathcal{E}_\mu^\rho$  grows.

**Example 3.1.** Consider the double-well potential  $\beta(x) := (x^2 - 1)^2 + c$  with  $c > 0$ . Let  $L = 2\pi$ ,  $\omega = 1$ ,  $\nu = 0$ , and  $c_0 \neq 1$ . Take  $\theta_0 := \theta_c = s$  and  $\rho_0 := \sin s$ . Then, for the solution  $(\theta, \rho)$  of (1.6), an elementary computation yields  $\lambda_{\theta 1}(0) = \lambda_{\theta 2}(0) = \lambda_\rho(0) = 0$  and

$$\begin{aligned} \frac{d}{dt} \mathcal{E}^\theta(\theta, \rho) \Big|_{t=0} &= (1 - c_0)^2 \int_0^{2\pi} \left( \frac{\mu}{2} \beta'(\rho_0) \partial_s^2 \rho_0 - (\partial_s(\beta(\rho_0)))^2 \right) \, ds - \frac{(1 - c_0)^4}{4} \int_0^{2\pi} (\beta'(\rho_0))^2 \, ds \\ &= \frac{\pi}{2} (1 - c_0)^2 \left( \mu - (1 - c_0)^2 - \frac{5}{2} \right), \end{aligned}$$

which is positive for  $\mu > (1 - c_0)^2 + \frac{5}{2}$ . On the other hand,

$$\frac{d}{dt} \mathcal{E}_\mu^\rho(\rho) \Big|_{t=0} = (1 - c_0)^2 \frac{\mu}{2} \int_0^{2\pi} \beta'(\rho_0) \partial_s^2 \rho_0 \, ds - \mu^2 \int_0^{2\pi} (\partial_s^2 \rho_0)^2 \, ds = \mu \pi \left( \frac{1}{2} (1 - c_0)^2 - \mu \right)$$

is positive for  $\mu < \frac{1}{2}(1 - c_0)^2$ . For numerical examples, see Figures 6, 8 and 9.

**Remark 3.2.** In view of Proposition 2.6 and Corollary 2.8, for  $\mu$  large,  $\mathcal{E}_\mu^\rho$  can be seen as the dominant term in  $\mathcal{E}_\mu$ . However, even for arbitrary large  $\mu$ ,  $\mathcal{E}_\mu^\rho$  might still not be monotonically decreasing. This can be seen with the evolution equations in (1.6). Indeed, taking  $\rho_0 \equiv \nu$  yields  $\mathcal{E}_\mu^\rho(\rho_0) = 0$ . On the other hand,  $\partial_t \rho|_{t=0} \neq 0$  for all  $\mu > 0$  as long as  $\theta$  is not constant and  $\beta'(\nu) \neq 0$ .

**3.2. Zeros of the curvature.** Differentiating (1.6) we find that the curvature  $\kappa = \partial_s \theta$  satisfies

$$(3.2) \quad \partial_t \kappa = \beta(\rho) \partial_s^2 \kappa + 2 \partial_s(\beta(\rho)) \partial_s \kappa + \partial_s^2(\beta(\rho)) \kappa + (\lambda_{\theta 1} \cos \theta + \lambda_{\theta 2} \sin \theta) \kappa - \partial_s^2(\beta(\rho)) c_0.$$

The structure of this evolution equation already indicates that the behavior of  $\kappa$  strongly depends on  $c_0$ . In case  $c_0 = 0$ , (3.2) may be written as a linear second order parabolic equation for  $\kappa$ . Indeed, we have

$$(3.3) \quad \partial_t \kappa = a \partial_s^2 \kappa + b \partial_s \kappa + c \kappa,$$

where we define the nonconstant coefficients  $a := \beta(\rho) > 0$ ,  $b := 2 \partial_s(\beta(\rho))$  and  $c := \partial_s^2(\beta(\rho)) + \lambda_{\theta 1} \cos \theta + \lambda_{\theta 2} \sin \theta$ . This allows us to use the techniques in [3] to study the evolution of the zero-set of the curvature. Sign-changing zeros of the curvature are *inflection points* of the curve, i.e. points where the curve locally changes from being convex to being concave or vice versa. Zeros at which the curvature does not change sign are called *undulation points* of the curve. First, we do not distinguish between inflection points and undulation points and show that the total number of zeros of  $\kappa$  decreases. In [38, Remark 3.2], this idea was also indicated, without proof, for the  $L^2$ -gradient flow of the angle function of the classical elastic energy without density-modulated stiffness.

For all  $t \geq 0$ , we denote by  $z_\kappa(t) \in \mathbb{N}_0 \cup \{\infty\}$  the number of zeros in  $[0, L)$  of the curvature  $\kappa(t, \cdot)$  of the global solution of (1.6). First we note the following.

**Lemma 3.3** ([3, Theorem C, (a)]). *Let  $c_0 = 0$  and  $(\theta, \rho)$  be the global solution of (1.6). Then  $z_\kappa(t)$  is finite for any  $t > 0$ .*

Further, the number of zeros of the curvature (inflection points and undulation points) does not increase along the evolution.

**Proposition 3.4.** *Let  $c_0 = 0$  and  $(\theta, \rho)$  be the global solution of (1.6). Then  $z_\kappa$  is a nonincreasing function on  $[0, \infty)$ .*

*Proof.* Consider the smooth  $L$ -periodic extension of  $\kappa = \partial_s \theta$  to  $\mathbb{R}$ , which we do not rename for simplicity. The function  $z_\kappa$  still denotes the number of zeros of the curvature in the interval  $[0, L)$ .

Let  $t_2 > 0$ . By Lemma 3.3, there exists  $n \in \mathbb{N}_0$  such that  $z_\kappa(t_2) = n$ . Without loss of generality, we assume that  $n \geq 1$ . Let  $0 \leq s_1 < s_2 < \dots < s_n < L$  be the zeros of  $\kappa$  at time  $t_2$ . By [3, Lemma 5.5], there are continuous curves  $x_i(t)$ ,  $i = 1, \dots, n$  in the zero-set  $Z_\kappa = \{(t, s) \in (0, \infty) \times \mathbb{R} : \kappa(t, s) = 0\}$  defined for  $t \in (0, t_2]$  such that  $x_i(t_2) = s_i$ . Moreover, define  $x_{n+1}(t) := x_1(t) + L$ ,  $t \in (0, t_2]$ . Then  $x_{n+1}(t)$  is also in  $Z_\kappa$ .

For  $t_1 \in (0, \infty)$  with  $t_1 < t_2$ , [3, Lemma 5.3] tells us that if  $x_i(t_2) < x_j(t_2)$ , then  $x_i(t) < x_j(t)$  for all  $t \in [t_1, t_2]$ ,  $i, j = 1, \dots, n+1$ . Hence, considering  $I_t := [x_1(t), x_{n+1}(t)]$  for  $t \in [t_1, t_2]$ , we find  $x_i(t) \in I_t$  for  $t \in [t_1, t_2]$  and  $i = 1, \dots, n$ . Thus, there are at least  $n$  zeros of  $\kappa$  on  $\{t_1\} \times I_t$ . Since by periodicity, the number of zeros on  $\{t_1\} \times [0, L)$  equals the number of zeros on  $\{t_1\} \times I_t$ , it follows that  $z_\kappa$  is nonincreasing on  $(0, \infty)$ .

It remains to consider the transition from  $t = 0$  to positive times. Due to Lemma 3.3 we assume without loss of generality that  $z_\kappa(0) < \infty$ . Similarly as in [3, Lemma 5.2] it follows that  $\lim_{t \searrow 0} x_i(t)$  exists for  $i = 1, \dots, n$ . Suppose that  $\lim_{t \searrow 0} x_i(t) = \lim_{t \searrow 0} x_j(t)$  for  $i < j$  and consider the nonempty open set  $G := \{(t, s) : 0 < t < t_2, x_i(t) < s < x_j(t)\}$ . Since  $\kappa \equiv 0$  on the parabolic boundary of  $G$ , the parabolic maximum principle implies that  $\kappa \equiv 0$  in  $G$ . This contradicts Lemma 3.3. Thus,  $\lim_{t \searrow 0} x_i(t) \neq \lim_{t \searrow 0} x_j(t)$  for  $i \neq j$  and it follows that  $z_\kappa(0) \geq n$ .  $\square$

In the following, we specifically consider the inflection points and show that the number of sign-changing zeros of  $\kappa$  does not increase. This means geometrically that the number of ‘dents’ of

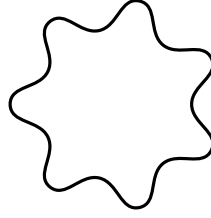


FIGURE 1. Curve with dents.

a curve like in Figure 1 is not increasing along the evolution. This is supported by numerical experiments, see Figure 9, while for  $c_0 \neq 0$ , Figure 6 gives an example for growing number of inflection points.

We denote the number of sign-changing zeros in  $[0, L]$  of the  $L$ -periodic extension of  $\kappa(t, \cdot)$  by  $\bar{z}_\kappa(t) \in \mathbb{N}_0 \cup \{\infty\}$ ,  $t \in [0, \infty)$ .

**Proposition 3.5.** *Let  $c_0 = 0$  and  $(\theta, \rho)$  be the global solution of (1.6). Then  $\bar{z}_\kappa$  is a nonincreasing function on  $[0, \infty)$ .*

*Proof.* Consider the smooth  $L$ -periodic extension of  $(\kappa, \rho)$  to  $\mathbb{R}$ . First we observe, that the zeros of  $\tilde{\kappa}(t, s) := e^{-\lambda t} \kappa(t, s)$ ,  $\lambda \in \mathbb{R}$ ,  $(t, s) \in [0, \infty) \times \mathbb{R}$ , coincide with the zeros of  $\kappa(t, \cdot)$ . By choosing  $\lambda$  sufficiently large, we can thus assume that  $\kappa$  satisfies (3.3) with  $c(t, s) < 0$  on  $[0, \infty) \times \mathbb{R}$ .

Let  $0 \leq t_1 < t_2 < \infty$ . By Lemma 3.3, there is  $n \in \mathbb{N}_0$  such that  $z_\kappa(t_2) = n$ . In view of Proposition 3.4 and due to periodicity of  $\kappa$ , we may assume without loss of generality that  $n > 1$ . As in the proof of Proposition 3.4, let  $0 \leq s_1 < \dots < s_n < L$  be such that  $\kappa(t_2, s_i) = 0$ ,  $i = 1, \dots, n$ . By the arguments in the proof of Proposition 3.4, there exist continuous curves  $x_i(t)$  in the zero-set of  $\kappa$  defined for  $t \in [0, t_2]$  such that  $x_i(t_2) = s_i$ ,  $i = 1, \dots, n$ , and  $x_i(t) < x_{i+1}(t)$  for  $t \in [0, t_2]$ , where  $x_{n+1} := x_1 + L$ .

Let  $i \in \{1, \dots, n\}$ . Either  $\kappa(t_2, \cdot) < 0$  or  $\kappa(t_2, \cdot) > 0$  on  $(x_i(t_2), x_{i+1}(t_2))$ . We assume the latter. Consider the open set  $G := \{(t, s) : t_1 < t < t_2, x_i(t) < s < x_{i+1}(t)\}$ , whose boundary is composed of the curves  $x_i, x_{i+1}$  and two vertical lines at  $t = t_1, t_2$ . By assumption and continuity,  $\kappa$  attains a positive maximum on  $\bar{G}$ , more precisely at the parabolic boundary by the maximum principle. But since  $\kappa(t, x_i(t)) = 0$  for  $t \in [t_1, t_2]$  and similarly for  $x_{i+1}$ , the maximum is attained at the vertical line  $t = t_1$ . Consequently, there exists an interval  $I \subset (x_i(t_1), x_{i+1}(t_1))$  with  $\kappa(t_1, s) > 0$  for  $s \in I$ . Thus, for each of the disjoint intervals  $(x_i(t_2), x_{i+1}(t_2))$ ,  $i = 1, \dots, n$ , with  $\kappa > 0$  (or  $\kappa < 0$ ), there is an interval in  $(x_i(t_1), x_{i+1}(t_1))$  with  $\kappa > 0$  (or  $\kappa < 0$ ). Since  $x_i(t) < x_{i+1}(t)$ ,  $t \in [t_1, t_2]$ , there are at least as many sign changes of  $\kappa$  in  $[x_1(t_1), x_1(t_1) + L]$  as in  $[x_1(t_2), x_1(t_2) + L]$ . By periodicity, it follows that  $\bar{z}_\kappa(t_1) \geq \bar{z}_\kappa(t_2)$ .  $\square$

*Proof of Theorem 1.2.* The result directly follows from Proposition 3.4 and Proposition 3.5.  $\square$

**3.3. Convexity.** In the following, we will use (3.3) to examine whether nonnegativity (or non-positivity) of the curvature of the initial curve is preserved along the evolution. This is closely related to convexity of the associated curve, see Remark 3.6 below.

*Proof of Theorem 1.3.* Case (ii) follows from Proposition 3.4. For case (i), we now show that if  $\partial_s \theta_0 \geq 0$ , then  $\partial_s \theta \geq 0$  for all  $t \in (0, \infty)$ . The proof for the nonpositive case works analogously. We consider the  $L$ -periodic extension of the global solution  $(\theta, \rho)$  to all of  $\mathbb{R}$ , which we do not rename for simplicity. Note that  $\partial_s \theta \in C^\infty((0, \infty) \times \mathbb{R})$  and  $\rho \in C^\infty((0, \infty) \times \mathbb{R})$  by Theorem 1.1. Since  $c_0 = 0$ ,  $\kappa$  satisfies (3.3) on  $(0, \infty) \times \mathbb{R}$ . Even though  $\theta$  itself is not even continuous on  $\mathbb{R}$ , due to the boundary condition  $\theta(L) - \theta(0) = 2\pi\omega$ , the coefficients  $a, b$  and  $c$  in (3.3) are smooth

on  $\mathbb{R}$  for all  $t \geq 0$ . Moreover, since the initial datum is attained in the  $C^2([0, L])$ -norm (see Theorem 1.1) and  $c$  is bounded globally in  $(0, \infty) \times \mathbb{R}$  (see [10, Section 4]), there is  $K > 0$  such that  $\sup_{t \in [0, \infty), s \in \mathbb{R}} c(t, s) < K$ . Defining  $\kappa_\varepsilon := \kappa + \varepsilon \exp(Kt)$  for  $\varepsilon > 0$  it follows that

$$(3.4) \quad \partial_t \kappa_\varepsilon > a(t, s) \partial_s^2 \kappa_\varepsilon + b(t, s) \partial_s \kappa_\varepsilon + c(t, s) \kappa_\varepsilon \quad \text{on } (0, \infty) \times \mathbb{R}$$

and  $\min_{s \in \mathbb{R}} \kappa_\varepsilon(0, s) = \min_{s \in [0, L]} \partial_s \theta_0(s) + \varepsilon > 0$ . Now we set

$$t^* := \sup \{t \geq 0 : \min_{s \in \mathbb{R}} \kappa_\varepsilon(\tau, s) > 0 \text{ for all } \tau \in (0, t)\}.$$

Clearly,  $t^* > 0$ . We assume that  $t^* < \infty$ . This implies that there is  $s^* \in \mathbb{R}$  such that

$$(3.5) \quad 0 = \min_{s \in \mathbb{R}} \kappa_\varepsilon(t^*, s) = \kappa_\varepsilon(t^*, s^*).$$

The necessary conditions for a local minimum yield  $\partial_s^2 \kappa_\varepsilon(t^*, s^*) \geq 0$ ,  $\partial_s \kappa_\varepsilon(t^*, s^*) = 0$  and  $\partial_t \kappa_\varepsilon(t^*, s^*) \leq 0$ . Together with (3.5) this is a contradiction to (3.4). Hence,  $\kappa_\varepsilon > 0$  on  $(0, \infty) \times \mathbb{R}$ . Sending  $\varepsilon \rightarrow 0$  yields  $\partial_s \theta = \kappa \geq 0$  on  $(0, \infty) \times \mathbb{R}$ .  $\square$

**Remark 3.6.** A planar closed curve  $\gamma$  is called convex if it is *simple* and its curvature  $\kappa = \partial_s \theta$  does not change sign. This is equivalent to  $\gamma$  parametrizing the boundary of a convex subset of  $\mathbb{R}^2$ . If the initial datum  $\theta_0$  of the flow (1.6) describes a convex curve and if  $c_0 = 0$ , then the corresponding curve remains convex for all times. Indeed, by Theorem 1.3, the sign of  $\kappa_0 = \partial_s \theta_0$  is preserved. Since the initial curve is simple and the winding number is preserved along the flow, we have  $\omega = \pm 1$  for all  $t \geq 0$  by Hopf's Umlaufsatz. Thus,  $\int_0^L |\kappa(t, s)| ds = 2\pi$  for any  $t \geq 0$ . Fenchel's Theorem yields that the evolving curve remains convex for all  $t \geq 0$ , in particular it remains simple.

For  $c_0 = 0$ , this is a distinctive advantage of the second order system (1.6) over the classical fourth order elastic flow, as simple curves generically can become nonsimple, see [32].

Remarkably, the statement of Theorem 1.3 can, in general, not be extended to the case  $c_0 \neq 0$ . We give an example with  $|c_0| > 0$  arbitrarily small. For a numerical example, see Figure 6.

**Example 3.7.** Let  $c_0 \neq 0$ . If  $c_0 > 0$ , let  $\beta'' > 0$  on  $[r, R]$  for some  $r, R \in \mathbb{R}$ . Otherwise, let  $\beta'' < 0$  on  $[r, R]$ . We consider an initial curve consisting of a straight line smoothly connected to the rest of the curve in such a way that  $\partial_s \theta_0 \geq 0$  on  $[0, L]$ . For example, a cigar-shaped curve as shown in Figure 2A. Let  $[a, b] \subset [0, L]$ ,  $a < b$ , such that

$$\kappa_0(s) = \partial_s \theta_0(s) = 0, \quad \rho_0(s) \in (r, R), \quad \partial_s \rho_0(s) \neq 0, \quad \partial_s^2 \rho_0(s) = 0 \quad \text{for } s \in [a, b],$$

cf. Figure 2B. Then (3.2) gives  $\partial_t \kappa(t, s)|_{t=0} = -\beta''(\rho_0(s))(\partial_s \rho_0(s))^2 c_0 < 0$  for  $s \in [a, b]$ . Thus,  $\kappa$  becomes negative on  $[a, b]$  for  $t > 0$  instantaneously and for any  $c_0$ .

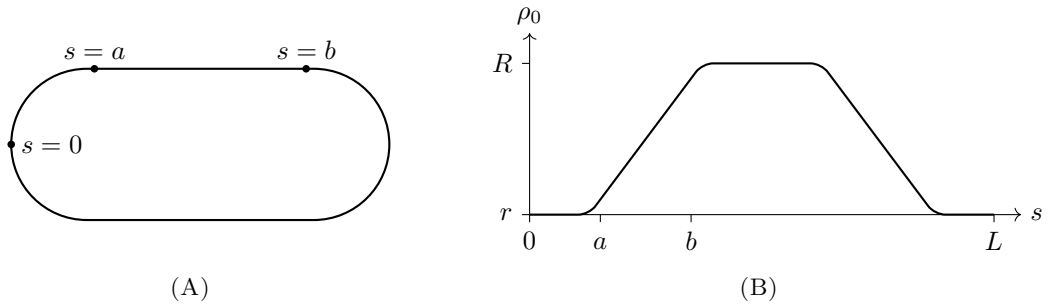


FIGURE 2. Cigar-shaped curve (A) with linear density on  $[a, b]$  (B).

**3.4. Nonnegativity of the density.** For a physical mass density  $\rho$ , only a positive sign is meaningful. We state a condition on  $\beta$  which gives a lower bound on  $\rho$  and particularly enables us to control its sign. Compared to the situation of Theorem 1.3, the evolution equation for  $\rho$  in (1.6) is not linear in  $\rho$ . This asks for stricter assumptions on  $\beta$ , which we again show to be sharp, see Example 3.10.

**Proposition 3.8.** *Let  $x_0 \in \mathbb{R}$ . Let  $\beta \in C^\infty(\mathbb{R})$  be such that  $\beta' \geq 0$  on  $[x_0, \infty)$  and  $\beta'(x_0) = 0$ . Let  $(\theta, \rho)$  be the global solution of (1.6) with admissible initial datum  $(\theta_0, \rho_0)$ . If  $\rho_0 \geq x_0$  on  $[0, L]$ , then  $\rho \geq x_0$  on  $(0, \infty) \times [0, L]$ .*

*Proof.* As in the proof of Theorem 1.3, consider the  $L$ -periodic extension of the global solution  $(\theta, \rho)$  to all of  $\mathbb{R}$ . Since  $\beta'(x_0) = 0$ , the function

$$f(x) := \begin{cases} \frac{\beta'(x)}{x - x_0} & \text{for } x \neq x_0, \\ \beta''(x) & \text{for } x = x_0 \end{cases}$$

is continuous. Choose  $R > 0$  such that  $\sup_{t \in [0, \infty), s \in \mathbb{R}} |\rho| < R$  and  $K > 0$  such that

$$(3.6) \quad \sup_{t \in [0, \infty), s \in \mathbb{R}} \left( \left( \sup_{x \in [-R, R]} |\beta''(x)| - f(\rho(t, s)) \right) (\partial_s \theta(t, s) - c_0)^2 \right) < 2K.$$

Let  $\varepsilon, T > 0$  be arbitrary. Define  $\rho_\varepsilon := \rho - x_0 + \varepsilon \exp(Kt)$  and

$$t^* := \sup \{t \in [0, T] : \min_{s \in \mathbb{R}} \rho_\varepsilon(\tau, s) > 0 \text{ for all } \tau \in (0, t)\}.$$

We assume that  $t^* < T$ . Observe that with (1.6) and (1.9),

$$(3.7) \quad \begin{aligned} \partial_t \rho_\varepsilon &= \mu \partial_s^2 \rho_\varepsilon - \frac{1}{2} f(\rho) (\partial_s \theta - c_0)^2 \rho_\varepsilon + \frac{1}{2} f(\rho) (\partial_s \theta - c_0)^2 \varepsilon e^{Kt} + K \varepsilon e^{Kt} \\ &\quad + \frac{1}{2L} \int_0^L \beta'(\rho_\varepsilon + x_0) (\partial_s \theta - c_0)^2 ds + \frac{1}{2L} \int_0^L (\beta'(\rho) - \beta'(\rho_\varepsilon + x_0)) (\partial_s \theta - c_0)^2 ds. \end{aligned}$$

For  $t \in [0, t^*]$ ,  $\rho_\varepsilon(t, s) + x_0 \geq x_0$  on  $\mathbb{R}$  and hence  $\beta'(\rho_\varepsilon(t, s) + x_0) \geq 0$ . Thus, the first integral in (3.7) has positive sign. Choosing  $\varepsilon$  so small that  $\sup_{t \in [0, T], s \in \mathbb{R}} (\rho + \varepsilon e^{Kt}) \leq R$ , we estimate the second integral in (3.7) for  $t \in [0, t^*]$  by

$$\frac{1}{2L} \int_0^L (\beta'(\rho) - \beta'(\rho_\varepsilon + x_0)) (\partial_s \theta - c_0)^2 ds \geq -\frac{1}{2} \sup_{[-R, R]} |\beta''| \varepsilon e^{Kt} \sup_{t \in [0, \infty), s \in \mathbb{R}} (\partial_s \theta - c_0)^2.$$

Thus it follows with the definition of  $K$  in (3.6) that for  $t \in [0, t^*]$ ,

$$\partial_t \rho_\varepsilon > \mu \partial_s^2 \rho_\varepsilon - \frac{1}{2} f(\rho) (\partial_s \theta - c_0)^2 \rho_\varepsilon.$$

Arguing as in the proof of Theorem 1.3 we find  $t^* = T$ , which implies that  $\rho_\varepsilon \geq 0$  on  $[0, T] \times \mathbb{R}$ . The limit  $\varepsilon \rightarrow 0$  yields  $\rho \geq x_0$  on  $[0, T] \times \mathbb{R}$ . Since  $T$  was chosen arbitrarily, the claim follows.  $\square$

**Remark 3.9.** With the same arguments it can be shown that for  $\beta \in C^\infty(\mathbb{R})$  such that  $\beta' \leq 0$  on  $(-\infty, x_0]$  and  $\beta'(x_0) = 0$  for some  $x_0 \in \mathbb{R}$ ,  $\rho_0 \leq x_0$  on  $[0, L]$  implies that  $\rho \leq x_0$  on  $(0, \infty) \times [0, L]$ .

The following example shows that it is necessary to impose some conditions on  $\beta$  in order to control the sign of  $\rho$ .

**Example 3.10.** Let  $x_0, R \in \mathbb{R}$ ,  $x_0 > R$  and suppose that  $\beta'(x_0) \geq \beta'(x)$  for all  $x \in [x_0, R]$ . Assume  $\omega \neq 0$  and  $c_0 \neq \frac{2\pi\omega}{L}$ . Consider an admissible initial datum with

$$\kappa_0 \equiv \frac{2\pi\omega}{L}, \quad x_0 \leq \rho_0 \leq R, \quad \rho_0 \equiv x_0 \text{ on } [a, b], \quad \rho \not\equiv x_0 \text{ on } [0, L]$$

for some nontrivial  $[a, b] \subset [0, L]$ . For  $s \in [a, b]$ , (1.6) and (1.9) imply

$$\partial_t \rho(t, s)|_{t=0} = -\frac{1}{2} \left( \frac{2\pi\omega}{L} - c_0 \right)^2 \left( \beta'(x_0) - \frac{1}{L} \int_0^L \beta'(\rho_0(s)) \, ds \right) < 0.$$

Thus, on  $[a, b]$  the density is not bounded from below by  $x_0$  for  $t > 0$ .

**3.5. Embeddedness.** We now discuss the (non)preservation of embeddedness. The curve  $\gamma$  described by the angle function  $\theta$  will no longer satisfy a second order parabolic equation (not even one with Lagrange multipliers), but a nonstandard integro-differential equation instead. Indeed, if  $\theta$  evolves according to (1.6), we may integrate (1.3) to describe the evolution of  $\gamma$ . Denoting by  $n = (-\sin \theta, \cos \theta)$  the usual normal vector field along  $\gamma$ , by integration by parts we find

$$\partial_t \gamma = \beta(\rho) (\partial_s^2 \gamma - c_0 n) + \int_0^s \partial_s \gamma \beta(\rho) \kappa (\kappa - c_0) \, dr + \int_0^s n (\lambda_{\theta 1} \sin \theta - \lambda_{\theta 2} \cos \theta) \, dr + v(t).$$

Here  $v(t) \in \mathbb{R}^2$  attributes for  $\partial_t \gamma(t, 0)$  and the boundary term arising at  $s = 0$ . Note that the second term on the right hand side still contains  $\kappa$ , a term of order two, in a nonlocal way. While it is possible to express  $\theta$  and thus the right hand side entirely in terms of  $\gamma$  and its derivatives, the resulting evolution equation is rather complicated and of nonstandard structure.

In particular, in contrast to the curve shortening flow (cf. [19]), we cannot rely on classical maximum principles to show the preservation of embeddedness. Instead, we use a recent energy-based argument [32] to conclude preservation of embeddedness for explicitly small initial energy. Note that  $\omega = \pm 1$  for any embedded curve by Hopf's Umlaufsatz.

**Proposition 3.11.** *Let  $C_{2T} \approx 146.628$  be as in [32, Theorem 1.1]. Let  $(\theta, \rho)$  be the global solution of (1.6) with admissible initial datum  $(\theta_0, \rho_0)$ . Suppose that  $\theta_0$  describes an embedded curve with rotation index  $\omega = 1$  and  $(\theta_0, \rho_0)$  satisfies*

$$(3.8) \quad \mathcal{E}_\mu(\theta_0, \rho_0) \leq \frac{\inf_{\mathbb{R}} \beta}{2} \left( \frac{C_{2T}}{L} - 4\pi c_0 + L c_0^2 \right).$$

*Then  $\theta(t, \cdot)$  describes an embedded curve for all  $t > 0$ .*

**Remark 3.12.** If  $\inf_{\mathbb{R}} \beta > 0$ , then the above threshold is nontrivial, i.e. there exist an admissible initial datum  $(\theta_0, \rho_0)$  satisfying (3.8). Indeed let  $\omega = 1$ ,  $\varepsilon > 0$  and let  $\nu \in \mathbb{R}$  such that  $\beta(\nu) \leq \inf_{\mathbb{R}} \beta + \varepsilon$ . Consider  $\rho_0 \equiv \nu$  and let  $\theta_0(s) = \frac{2\pi s}{L}$ . Then, we have

$$\mathcal{E}_\mu(\theta_0, \rho_0) = \frac{\beta(\nu)}{2} \left( \frac{4\pi^2}{L} - 4\pi c_0 + L c_0^2 \right).$$

Using that  $4\pi^2 < C_{2T}$  it follows that the assumptions of Proposition 3.11 are satisfied for  $\varepsilon > 0$  small enough. Moreover,  $4\pi^2 < C_{2T}$  also yields that the right hand side of (3.8) is positive if  $\inf_{\mathbb{R}} \beta > 0$ .

*Proof of Proposition 3.11.* Let  $t > 0$ . If  $(\theta_0, \rho_0)$  is stationary, then there is nothing to show. Thus, by (3.1), we may assume that the energy is strictly decreasing, i.e.  $\mathcal{E}_\mu(\theta(t, \cdot), \rho(t, \cdot)) < \mathcal{E}_\mu(\theta_0, \rho_0)$ . Moreover, (3.1) and the assumption yield that

$$\int_0^L \kappa(t, s)^2 \, ds \leq \frac{2}{\inf_{\mathbb{R}} \beta} \mathcal{E}_\mu(\theta(t, \cdot), \rho(t, \cdot)) + 4\pi c_0 - L c_0^2 < \frac{2}{\inf_{\mathbb{R}} \beta} \mathcal{E}_\mu(\theta_0, \rho_0) + 4\pi c_0 - L c_0^2 \leq \frac{C_{2T}}{L}.$$

Now,  $\theta(t, \cdot)$  describes a closed curve with rotation index one, and hence this curve must be embedded by [32, Theorem 1.4].  $\square$

**3.6. Symmetry.** The following section is inspired by [27]. We restrict ourselves here to  $\omega = 1$ .

3.6.1. *Rotational symmetry.* Without further comment, in this section, we frequently identify  $(\theta - \phi, \rho)$  with its  $L$ -periodic extension to  $\mathbb{R}$ . Here,  $\phi$  as in (2.1).

**Definition 3.13.** Let  $\omega = 1$ ,  $(\theta, \rho) \in C^\infty([0, L])$  and  $k \in \mathbb{N}$  with  $k \geq 2$ . If  $(\theta - \phi, \rho)$  is  $\frac{L}{k}$ -periodic, we call the heterogeneous curve described by  $(\theta, \rho)$   $k$ -fold rotationally symmetric.

**Remark 3.14.** We gather some immediate consequences of rotational symmetry.

(i) The  $\frac{L}{k}$ -periodicity of  $\theta - \phi$  is equivalent to demand that

$$(3.9) \quad \theta(s) = \theta\left(s - \frac{nL}{k}\right) + \frac{2\pi n}{k} \quad \text{for } s \in \left[\frac{nL}{k}, \frac{(n+1)L}{k}\right] \text{ and } n = 0, 1, \dots, k-1.$$

(ii) If  $\theta - \phi$  is  $\frac{L}{k}$ -periodic, then  $\theta$  describes a closed curve. Indeed, using (3.9) we have

$$\begin{aligned} \int_0^L \sin \theta(s) \, ds &= \sum_{n=0}^{k-1} \int_{\frac{nL}{k}}^{\frac{(n+1)L}{k}} \sin \theta(s) \, ds = \sum_{n=0}^{k-1} \int_{\frac{nL}{k}}^{\frac{(n+1)L}{k}} \sin\left(\theta\left(s - \frac{nL}{k}\right) + \frac{2\pi n}{k}\right) \, ds \\ &= \int_0^{\frac{L}{k}} \sum_{n=0}^{k-1} \sin\left(\theta(s) + \frac{2\pi n}{k}\right), \end{aligned}$$

which is zero for  $k \geq 2$  since

$$\sum_{n=0}^{k-1} \sin\left(\theta + \frac{2\pi n}{k}\right) = \text{Im}\left(\exp(i\theta) \sum_{n=0}^{k-1} \exp(i\frac{2\pi n}{k})\right) = \text{Im}\left(\exp(i\theta) \frac{1 - \exp(2\pi i)}{1 - \exp(\frac{2\pi i}{k})}\right) = 0.$$

Analogously, we obtain  $\int_0^L \cos \theta(s) \, ds = 0$ .

(iii) If  $(\theta, \rho) \in C^\infty([0, L])$  describes a  $k$ -fold rotationally symmetric heterogeneous curve and we choose

$$(3.10) \quad \gamma(0) := \frac{1}{L} \int_0^L s \begin{pmatrix} \cos \theta(s) \\ \sin \theta(s) \end{pmatrix} \, ds$$

(which ensures that  $\int_0^L \gamma(s) \, ds = 0$ ), a computation shows that for  $s \in \left[\frac{nL}{k}, \frac{(n+1)L}{k}\right]$  with  $n = 0, 1, \dots, k-1$ , we have

$$\text{Rot}\left(\frac{2\pi n}{k}\right) \gamma\left(s - \frac{nL}{k}\right) = \gamma(s).$$

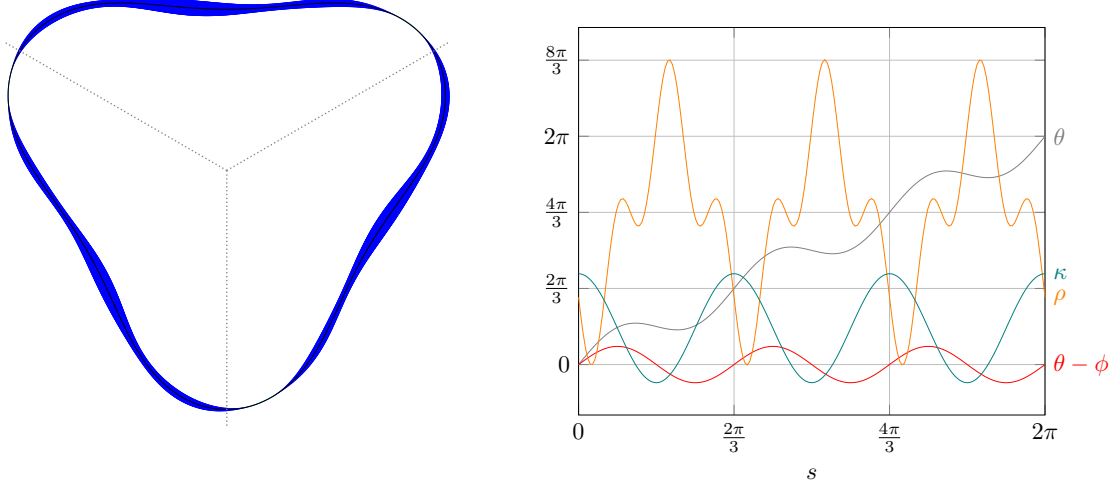
Here,  $\text{Rot}(\alpha)$  is the counterclockwise rotation by the angle  $\alpha$ . Since additionally  $\rho\left(s - \frac{nL}{k}\right) = \rho(s)$ , the graph of the heterogeneous curve described by  $(\theta, \rho)$  indeed possesses a  $k$ -fold rotational symmetry, see Figure 3.

We show that the flow (1.6) preserves  $k$ -fold rotational symmetry for all  $k \in \mathbb{N}$ ,  $k \geq 2$ .

**Proposition 3.15.** Let  $\omega = 1$  and  $k \geq 2$ . Let  $(\theta, \rho)$  be the solution of (1.6) with admissible initial datum  $(\theta_0, \rho_0)$ . If  $(\theta_0, \rho_0)$  describes a  $k$ -fold rotationally symmetric heterogeneous curve, then so does  $(\theta, \rho)$  for all  $t \in (0, \infty)$ .

*Proof.* We consider the  $L$ -periodic extension of  $(u, \rho) := (\theta - \phi, \rho)$  to  $\mathbb{R}$ . Notice that  $(u, \rho) \in C^\infty((0, \infty) \times \mathbb{R})$ . We define  $(\tilde{u}, \tilde{\rho}) \in C^\infty((0, \infty) \times \mathbb{R})$  by  $(\tilde{u}, \tilde{\rho})(t, s) := (u, \rho)(t, s - \frac{L}{k})$  and  $(\tilde{\theta}, \tilde{\rho}) \in C^\infty((0, \infty) \times \mathbb{R})$  by  $(\tilde{\theta}, \tilde{\rho}) := (\tilde{u} + \phi, \tilde{\rho})$ . Notice, that  $\tilde{\theta} \in C^\infty((0, \infty) \times \mathbb{R})$  is not periodic. Our intention now is to show that the restriction of  $(\tilde{\theta}, \tilde{\rho})$  to  $(0, \infty) \times [0, L]$  solves (1.6) with initial datum  $(\theta_0, \rho_0)$ . By uniqueness of the solution (see Theorem 1.1), it then follows that  $(\tilde{\theta} - \phi, \tilde{\rho}) = (\theta - \phi, \rho)$  and thus

$$(\theta - \phi, \rho)(t, s) = (\tilde{u}, \tilde{\rho})(t, s) = (u, \rho)\left(t, s - \frac{L}{k}\right) = (\theta - \phi, \rho)\left(t, s - \frac{L}{k}\right)$$

FIGURE 3. Example of a 3-fold rotationally symmetric configuration  $(\theta, \rho)$ .

for  $s \in \mathbb{R}$ . Thus, the heterogeneous curve described by  $(\theta, \rho)$  is  $k$ -fold rotationally symmetric. It is clear that  $(\tilde{\theta}, \tilde{\rho}) \in C^\infty((0, \infty) \times [0, L])$ . With (2.1) and the  $L$ -periodicity of  $u$ , we have

$$(3.11) \quad \begin{aligned} \tilde{\theta}(t, s) &= \tilde{u}(t, s) + \phi(s) = u(t, s - \frac{L}{k}) + \phi(s - \frac{L}{k}) + \phi(\frac{L}{k}) = \theta(t, s - \frac{L}{k}) + \frac{2\pi}{k} \\ &\quad \text{for } (t, s) \in (0, \infty) \times (\frac{L}{k}, L], \\ \tilde{\theta}(t, s) &= \theta(t, s - \frac{L}{k} + L) + \frac{2\pi}{k} - 2\pi \quad \text{for } (t, s) \in (0, \infty) \times [0, \frac{L}{k}]. \end{aligned}$$

Using this and trigonometric identities, we see that for  $t \geq 0$  and  $s \in [0, L]$ ,  $(\tilde{\theta}, \tilde{\rho})$  solves

$$(3.12) \quad \partial_t \tilde{\theta} = \partial_s (\beta(\tilde{\rho}) (\partial_s \tilde{\theta} - c_0)) + \alpha_1 \sin \tilde{\theta} - \alpha_2 \cos \tilde{\theta}$$

with  $\alpha_1 := \lambda_{\theta 1}(\theta, \rho) \cos(\frac{2\pi}{k}) - \lambda_{\theta 2}(\theta, \rho) \sin(\frac{2\pi}{k})$ ,  $\alpha_2 := \lambda_{\theta 1}(\theta, \rho) \sin(\frac{2\pi}{k}) + \lambda_{\theta 2}(\theta, \rho) \cos(\frac{2\pi}{k})$ . We use (3.11) and the fact that  $\theta$  describes a closed curve to obtain

$$\begin{aligned} \int_0^L \sin \tilde{\theta} \, ds &= \int_0^{\frac{L}{k}} \sin (\theta(s - \frac{L}{k} + L) + \frac{2\pi}{k}) \, ds + \int_{\frac{L}{k}}^L \sin (\theta(s - \frac{L}{k}) + \frac{2\pi}{k}) \, ds \\ &= \int_0^L \sin (\theta + \frac{2\pi}{k}) \, ds = \cos(\frac{2\pi}{k}) \int_0^L \sin \theta \, ds + \sin(\frac{2\pi}{k}) \int_0^L \cos \theta \, ds = 0 \end{aligned}$$

(cf. (1.7)) and  $\int_0^L \cos \tilde{\theta} \, ds = 0$  for all  $t \geq 0$ . In particular, this implies

$$(3.13) \quad \int_0^L \sin \tilde{\theta} \partial_t \tilde{\theta} \, ds = \int_0^L \cos \tilde{\theta} \partial_t \tilde{\theta} \, ds = 0.$$

Inserting (3.12) into (3.13) and comparing to (1.8), a short computation yields  $\alpha_1 = \lambda_{\theta 1}(\tilde{\theta}, \tilde{\rho})$  and  $\alpha_2 = \lambda_{\theta 2}(\tilde{\theta}, \tilde{\rho})$ . Moreover, we check that  $\lambda_\rho(\tilde{\theta}, \tilde{\rho}) = \lambda_\rho(\theta, \rho)$  and

$$\partial_t \tilde{\rho} = \mu \partial_s^2 \tilde{\rho} - \frac{1}{2} \beta'(\tilde{\rho}) (\partial_s \tilde{\theta} - c_0)^2 + \lambda_\rho(\tilde{\theta}, \tilde{\rho}).$$

Next, we notice that  $(\tilde{\theta}, \tilde{\rho})$  satisfies the boundary conditions

$$\tilde{\theta}(t, L) - \tilde{\theta}(t, 0) = \tilde{u}(t, L) + \phi(L) - \tilde{u}(t, 0) = u(t, L - \frac{L}{k}) + 2\pi - u(t, -\frac{L}{k}) = 2\pi,$$

$\tilde{\rho}(t, L) = \tilde{\rho}(t, 0)$ , and  $\partial_s(\tilde{\theta}, \tilde{\rho})(t, L) = \partial_s(\tilde{\theta}, \tilde{\rho})(t, 0)$  for all  $t > 0$ . Since  $(\theta_0 - \phi, \rho_0)$  describes a  $k$ -fold rotationally symmetric heterogeneous curve, we know with (3.11) and Remark 3.14 (i) that

$$\lim_{t \rightarrow 0} (\tilde{\theta}, \tilde{\rho})(t, s) = \lim_{t \rightarrow 0} \left( \theta(t, s - \frac{L}{k}) + \frac{2\pi}{k}, \rho(t, s - \frac{L}{k}) \right) = (\theta_0, \rho_0)(s)$$

(in  $C^{2+\alpha}([0, L])$  for all  $\alpha \in (0, 1)$ ) for  $s \in [\frac{L}{k}, L]$  and analogously for  $s \in [0, \frac{L}{k}]$ . Hence,  $(\tilde{\theta}, \tilde{\rho})$  solves (1.6) with initial datum  $(\theta_0, \rho_0)$ .  $\square$

A distinctive feature of rotationally symmetric configurations is that the Lagrange multipliers  $\lambda_{\theta 1}$  and  $\lambda_{\theta 2}$  vanish.

**Lemma 3.16.** *Let  $k \geq 2$  and let  $(\theta, \rho) \in C^\infty([0, L])$  describe a  $k$ -fold rotationally symmetric heterogeneous curve. Then  $\lambda_{\theta 1}(\theta, \rho) = \lambda_{\theta 2}(\theta, \rho) = 0$ .*

*Proof.* With the  $\frac{L}{k}$ -periodicity of  $\rho$  and with (3.9) we obtain that

$$\int_0^L \begin{pmatrix} -\sin \theta \\ \cos \theta \end{pmatrix} \partial_s (\beta(\rho)(\partial_s \theta - c_0)) \, ds = \sum_{n=0}^{k-1} \int_0^{\frac{L}{k}} \begin{pmatrix} -\sin \left( \theta + \frac{2\pi n}{k} \right) \\ \cos \left( \theta + \frac{2\pi n}{k} \right) \end{pmatrix} \partial_s (\beta(\rho)(\partial_s \theta - c_0)) \, ds.$$

This sum is zero as we have seen in Remark 3.14 (ii). With (1.8), this yields  $\lambda_{\theta 1} = \lambda_{\theta 2} = 0$ .  $\square$

The vanishing of  $\lambda_{\theta 1}$  and  $\lambda_{\theta 2}$  gives the following extension of Lemma 2.11. If  $\omega = 1$ ,  $c_0 \neq \frac{2\pi}{L}$  and  $(\theta, \rho)$  is a constrained critical point with constant curvature, which describes a  $k$ -fold rotationally symmetric configuration, then  $\mathcal{L}^1(\{x : \beta'(x) = 0\}) = 0$  implies  $\rho \equiv \nu$ .

Furthermore, Lemma 3.16 together with Proposition 3.15 enables us to prove Theorem 1.4.

*Proof of Theorem 1.4.* With Proposition 3.15 we know that the solution  $(\theta - \phi, \rho)$  remains  $\frac{L}{k}$ -periodic for all  $t \geq 0$ . Hence, Lemma 3.16 implies that  $\lambda_{\theta 1}(t) = \lambda_{\theta 2}(t) = 0$  for all  $t \geq 0$ . This is why (3.2) can be written as

$$(3.14) \quad \partial_t(\kappa - c_0) = \beta(\rho) \partial_s^2(\kappa - c_0) + 2\partial_s(\beta(\rho)) \partial_s(\kappa - c_0) + \partial_s^2(\beta(\rho))(\kappa - c_0).$$

Since (3.14) has the same structure as (3.3), we can proceed as in the proof of Theorem 1.3 to show the claim.  $\square$

In Example 3.7, we saw that convexity may not be preserved for  $c_0 \neq 0$ . With a small modification of the density, the example can be made rotationally symmetric, so that convexity ( $\kappa_0 \geq 0$ ) is still lost, while the bound  $\kappa_0 \geq c_0$  is preserved by Theorem 1.4.

**3.6.2. Axial symmetry.** We characterize axial symmetry of heterogeneous curves (after a possible shift in the  $s$ -argument) as follows.

**Definition 3.17.** Let  $(\theta, \rho) \in C^\infty([0, L])$ . We call the heterogeneous curve described by  $(\theta, \rho)$  *axially symmetric*, if

$$(3.15) \quad (\partial_s \theta, \rho)(s) = (\partial_s \theta, \rho)(L - s) \quad \text{for } s \in [0, L].$$

**Remark 3.18.** Axial symmetry implies the following properties.

(i) Integrating (3.15) we obtain the equivalent condition

$$(3.16) \quad \theta(s) = \theta(L) + \theta(0) - \theta(L - s) \quad \text{for } s \in [0, L].$$

(ii) Let  $(\theta, \rho) \in C^\infty([0, L])$  satisfy (3.15) and  $\gamma(0) \in \mathbb{R}^2$  be as in (3.10). A computation shows that

$$\text{Ref}\left(\theta(0) - \frac{\pi}{2}\right) \gamma(s) = \gamma(L - s),$$

where  $\text{Ref}(\alpha)$  represents the reflection about an axis through the origin with angle  $\alpha$  to the  $x$ -axis. Since additionally  $\rho(s) = \rho(L - s)$ , (3.15) indeed implies that the corresponding heterogeneous curve is axially symmetric, see Figure 4.

(iii) A short computation, relying on (3.16) and the preservation of the integral of the inclination angle [10, Lemma 2.3], implies that for a solution  $(\theta, \rho)$  describing an axially symmetric curve for all times  $t \geq 0$ , we have  $\theta(t, 0) = \theta_0(0)$ .

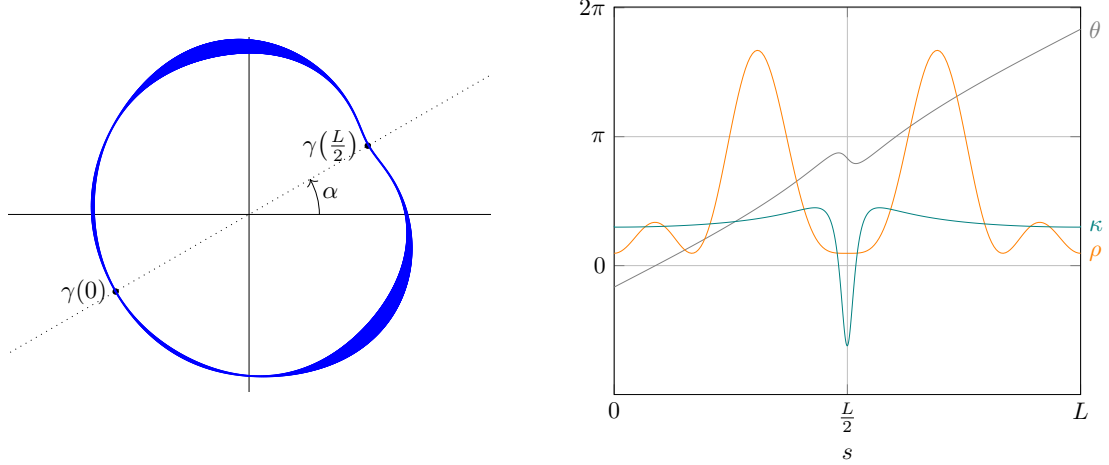


FIGURE 4. Example of an axially symmetric configuration  $(\theta, \rho)$ .

We show that if the initial datum describes an axially symmetric heterogeneous curve, then this also applies to the solution for all  $t > 0$ .

**Proposition 3.19.** *Let  $\omega = 1$  and  $(\theta, \rho)$  be the solution of (1.6) with admissible initial datum  $(\theta_0, \rho_0)$ . If  $(\theta_0, \rho_0)$  describes a heterogeneous curve which is axially symmetric, then so does  $(\theta, \rho)$  for all  $t \in (0, \infty)$ .*

*Proof.* Let  $(\theta, \rho)$  be the solution of (1.6) with initial datum  $(\theta_0, \rho_0)$ . We define

$$(\tilde{\theta}, \tilde{\rho})(t, s) := (\theta_0(L) + \theta_0(0) - \theta(t, L - s), \rho(t, L - s))$$

for  $(t, s) \in (0, \infty) \times [0, L]$  and show that  $(\tilde{\theta}, \tilde{\rho})$  solves (1.6) with the same initial datum  $(\theta_0, \rho_0)$ . By uniqueness of the solution, it follows that  $(\theta, \rho) = (\tilde{\theta}, \tilde{\rho})$  in  $[0, \infty) \times [0, L]$ . This yields  $(\partial_s \theta, \rho)(t, s) = (\partial_s \theta, \rho)(t, L - s)$  in  $[0, \infty) \times [0, L]$ . Thus,  $(\theta, \rho)$  describes an axially symmetric heterogeneous curve for all  $t > 0$ .

It is clear that  $(\tilde{\theta}, \tilde{\rho}) \in C^\infty((0, \infty) \times [0, L])$ . Since  $\partial_s \tilde{\theta}(s) = (\partial_s \theta)(L - s)$ ,  $\partial_s^2 \tilde{\theta} = -(\partial_s^2 \theta)(L - s)$  and  $\partial_s \tilde{\rho}(s) = -(\partial_s \rho)(L - s)$ , we see that

$$\partial_t \tilde{\theta} = \beta(\tilde{\rho}) \partial_s^2 \tilde{\theta} + \beta'(\tilde{\rho}) \partial_s \tilde{\rho} (\partial_s \tilde{\theta} - c_0) + \alpha_1 \sin \tilde{\theta} - \alpha_2 \cos \tilde{\theta}.$$

Here, we have  $\alpha_1(t) = \lambda_{\theta 1}(\theta, \rho) \cos(\theta_0(L) + \theta_0(0)) - \lambda_{\theta 2}(\theta, \rho) \sin(\theta_0(L) + \theta_0(0))$  and  $\alpha_2(t) = \lambda_{\theta 1}(\theta, \rho) \sin(\theta_0(L) + \theta_0(0)) + \lambda_{\theta 2}(\theta, \rho) \cos(\theta_0(L) + \theta_0(0))$  (by using trigonometric identities). Similarly,

$$\int_0^L \sin \tilde{\theta} \, ds = \sin(\theta_0(L) - \theta_0(0)) \int_0^L \cos \theta \, ds - \cos(\theta_0(L) - \theta_0(0)) \int_0^L \sin \theta \, ds = 0.$$

Analogously, we obtain  $\int_0^L \cos \tilde{\theta} \, ds = 0$ . Thus,  $\tilde{\theta}$  describes a closed curve. As in the proof of Proposition 3.15 one shows that this implies that  $\alpha_1 = \lambda_{\theta 1}(\tilde{\theta}, \tilde{\rho})$  and  $\alpha_2 = \lambda_{\theta 2}(\tilde{\theta}, \tilde{\rho})$ . Moreover,  $\lambda_{\rho}(\tilde{\theta}, \tilde{\rho}) = \lambda_{\rho}(\theta, \rho)$  and

$$\partial_t \tilde{\rho} = \mu \partial_s^2 \tilde{\rho} - \frac{1}{2} \beta'(\tilde{\rho}) (\partial_s \tilde{\theta} - c_0)^2 + \lambda_{\rho}(\tilde{\theta}, \tilde{\rho}).$$

It is readily checked that  $(\tilde{\theta}, \tilde{\rho})$  satisfies the boundary conditions in (1.6). Using that  $(\theta_0, \rho_0)$  describes an axially symmetric configuration, we further have

$$\lim_{t \rightarrow 0} (\tilde{\theta}, \tilde{\rho})(t, s) = (\theta_0(L) + \theta_0(0) - \theta_0(L-s), \rho_0(L-s)) = (\theta_0, \rho_0)(s)$$

(in  $C^{2+\alpha}([0, L])$  for all  $\alpha \in (0, 1)$ ). Hence,  $(\tilde{\theta}, \tilde{\rho})$  is a solution of (1.6) with initial datum  $(\theta_0, \rho_0)$  and the claim follows.  $\square$

**Remark 3.20.** The proof of Proposition 3.19 shows that for an axially symmetric initial datum  $(\theta_0, \rho_0)$ , the solution  $(\theta, \rho)$  keeps  $\theta(t, 0) = \theta_0(0)$  for all  $t \in [0, \infty)$ .

#### 4. ASYMPTOTIC BEHAVIOR

Since stationary solutions of (1.6) are precisely the constrained critical points (compare (2.4)–(2.5) with (1.10)), we can already derive some properties of the limit  $(\theta_{\infty}, \rho_{\infty})$  in Theorem 1.1 by using the classification of constrained critical points in Sections 2.2 and 2.3.

**4.1. Convergence to a homogeneous elastica under growth assumptions on  $\beta$ .** In this section, we impose some additional assumptions on the initial datum and the model parameters, under which the limit of (1.6) is a homogeneous elastica.

*Proof of Theorem 1.5.* With (1.6), (1.9), and integration by parts we have

$$(4.1) \quad \frac{d}{dt} \int_0^L (\rho - \nu)^2 \, ds = 2 \int_0^L \rho \partial_t \rho \, ds = -2\mu \int_0^L (\partial_s \rho)^2 \, ds + \int_0^L (\nu - \rho) \beta'(\rho) (\partial_s \theta - c_0)^2 \, ds.$$

We use (1.11) to estimate the second term on the right hand side of (4.1) and obtain

$$\begin{aligned} \frac{d}{dt} \int_0^L (\rho - \nu)^2 \, ds &\leq -2\mu \int_0^L (\partial_s \rho)^2 \, ds + \bar{C} \int_0^L (\nu - \rho)^2 \beta(\rho) (\partial_s \theta - c_0)^2 \, ds \\ &\leq -2\mu \int_0^L (\partial_s \rho)^2 \, ds + \bar{C} \sup_{s \in [0, L]} (\nu - \rho)^2 \int_0^L \beta(\rho) (\partial_s \theta - c_0)^2 \, ds \\ &\leq -2\mu \int_0^L (\partial_s \rho)^2 \, ds + 2L\bar{C}\mathcal{E}_{\mu}(\theta_0, \rho_0) \int_0^L (\partial_s \rho)^2 \, ds, \end{aligned}$$

using (3.1),  $\sup_{s \in [0, L]} |\nu - \rho| \leq \int_0^L |\partial_s \rho| \, ds$  and Cauchy–Schwarz. This yields

$$\frac{d}{dt} \int_0^L (\rho - \nu)^2 \, ds \leq -2 \left( \frac{2\pi}{L} \right)^2 (\mu - L\bar{C}\mathcal{E}_{\mu}(\theta_0, \rho_0)) \int_0^L (\rho - \nu)^2 \, ds.$$

By Gronwall's inequality we conclude that

$$\int_0^L (\rho - \nu)^2 \, ds \leq \left( \int_0^L \rho_0^2 \, ds - \nu^2 L \right) \exp \left( -\frac{8\pi^2}{L^2} (\mu - L\bar{C}\mathcal{E}_{\mu}(\theta_0, \rho_0)) t \right).$$

Since  $\bar{C}L\mathcal{E}_{\mu}(\theta_0, \rho_0) < \mu$ , it follows that  $\rho \rightarrow \nu$  in  $L^2(0, L)$  exponentially fast. By the subconvergence result in Theorem 1.1, there is a sequence  $t_n \rightarrow \infty$  and  $\theta_{\infty} \in C^{\infty}([0, L])$  such that  $(\theta_{\infty}, \rho_{\infty} = \nu)$  is a solution of (1.10) and  $\theta(t_n) \rightarrow \theta_{\infty}$  in  $C^2([0, L])$ . By Lemma 2.9, we find that  $(\theta_{\infty}, \rho_{\infty})$  describes a homogeneous elastica.

If  $\omega \neq 0$ , Lemma 2.4 yields that  $\theta_\infty$  describes an  $\omega$ -fold covering of a circle, so that necessarily  $\partial_s \theta_\infty = \frac{2\pi\omega}{L}$ . From [10, Lemma 2.3], we conclude that  $\int_0^L \theta_\infty \, ds = \int_0^L \theta_0 \, ds$ , which implies  $\theta_\infty(s) = \phi(s) + \frac{1}{L} \int_0^L \theta_0 \, ds - \pi\omega L$ ,  $s \in [0, L]$ . In particular,  $\theta_\infty$  does not depend on the sequence  $(t_n)_{n \in \mathbb{N}}$ , and statement (i) follows from a subsequence argument.

In the case  $\omega = 0$ , the analyticity assumption on  $\beta$  and Theorem 1.1 imply that  $(\theta(t), \rho(t)) \rightarrow (\theta_\infty, \rho_\infty = \nu)$  in  $C^2([0, L])$  as  $t \rightarrow \infty$ , where  $(\theta_\infty, \rho_\infty)$  satisfies (1.10). Again, Lemma 2.9 implies that  $\theta_\infty$  describes an elastica, so necessarily a multifold covered figure eight elastica by Lemma 2.4. Statement (ii) follows.  $\square$

The necessity for stronger assumptions in the case  $\omega = 0$  arises from the parametrization invariance of the energy, a general issue for geometric flows which occurs here despite working only with arclength parametrizations. Suppose that  $(\theta, \rho)$  is a solution to (1.6) and  $(\theta_\infty, \rho_\infty)$  is a solution to (1.10) originating from the subconvergence result in Theorem 1.1, i.e.  $(\theta_\infty, \rho_\infty) = \lim_{n \rightarrow \infty} (\theta(t_n), \rho(t_n))$  for some sequence  $t_n \rightarrow \infty$ . With  $\phi$  as in (2.1), we write  $\theta_\infty = u_\infty + \phi$ . Identifying  $u_\infty, \rho_\infty$  with their smooth  $L$ -periodic extensions to  $\mathbb{R}$ , we find that for any  $s_0 \in \mathbb{R}$ , the pair

$$(4.2) \quad (\hat{\theta}_\infty, \hat{\rho}_\infty)(s) = (\phi(s) + u_\infty(s - s_0), \rho_\infty(s - s_0)), \quad s \in [0, L],$$

is also stationary for any  $s_0 \in \mathbb{R}$ . In fact, any other arclength parametrization of the corresponding curve leads to an angle function of this form. In particular, the set of possible limits (i.e. solutions to (1.10)) is nondiscrete, so that Łojasiewicz–Simon gradient inequalities are generically needed for deducing convergence from subconvergence. Hence, it is somehow surprising that this argument is not needed in case (i) of Theorem 1.5. The reason for this is that if  $(\theta_\infty, \rho_\infty)$  describes a circle, then any reparametrization of the form (4.2) with  $s_0 \neq 0$  will result in adding a constant to the original angle function since  $\theta_\infty$  is affine. Since by [10, Lemma 2.3],  $\int_0^L \theta_\infty \, ds$  is determined by the initial datum, this degree of freedom is not present in the case  $\omega \neq 0$ , resulting in full convergence. On the curve level, adding a constant to  $\theta$  corresponds to a rotation of the associated curve about a fixed angle, i.e. for a circle there is a one-to-one correspondence between arclength reparametrizations and rotations.

On the other hand, in the case  $\omega = 0$ , the classification of solutions to the elastica equation in [28, Proposition 3.3] allows us to determine all the parameters, except for the invariance due to (4.2), see also [33, Proposition B.8]. Hence the Łojasiewicz inequality (and consequently analyticity of  $\beta$ , cf. [37, Corollary 6.3]) is necessary to ensure convergence.

For  $\omega = 1$ , we have dealt with rotational symmetry of solutions. In this case we can prove exponential convergence of the curvature to a constant if the length allows for a circle with curvature  $\kappa \equiv c_0$ .

**Proposition 4.1.** *Let  $\omega = 1$ ,  $c_0 = \frac{2\pi}{L}$ , and let  $(\theta_0, \rho_0) \in C^\infty([0, L])$  be an admissible initial datum describing a  $k$ -fold rotationally symmetric heterogeneous curve for some  $k \geq 2$ . Then, as  $t \rightarrow \infty$ , the solution  $(\theta, \rho)$  to (1.6) converges exponentially fast to  $(\theta_\infty, \rho_\infty)$  with  $\partial_s \theta_\infty \equiv c_0$ ,  $\rho_\infty \equiv \nu$ . In particular, the limit describes a circle with constant density.*

*Proof.* Let  $(\theta, \rho)$  be the solution to (1.6) and recall  $\mathcal{E}^\theta(t) = \frac{1}{2} \int_0^L \beta(\rho)(\kappa - c_0)^2 \, ds$  with  $\kappa = \partial_s \theta$ . Due to Proposition 3.15 and Lemma 3.16,  $\lambda_{\theta 1}(t) = \lambda_{\theta 2}(t) = 0$  for all  $t \geq 0$ . Thus

$$(4.3) \quad \begin{aligned} \frac{d}{dt} \mathcal{E}^\theta &= \frac{1}{2} \int_0^L \beta'(\rho) \partial_t \rho (\kappa - c_0)^2 \, ds + \int_0^L \beta(\rho) (\kappa - c_0) \partial_t \kappa \, ds \\ &\leq \frac{\sup_{(t,s)} |\beta'(\rho)|}{2 \inf_{(t,s)} (\beta(\rho))^2} \|\partial_t \rho\|_{L^\infty(0,L)} \int_0^L (\beta(\rho))^2 (\kappa - c_0)^2 \, ds - \int_0^L (\partial_s(\beta(\rho)(\kappa - c_0)))^2 \, ds \end{aligned}$$

Note that  $\sup_{(t,s) \in [0,\infty) \times [0,L]} |\beta'(\rho)| < \infty$  and  $\inf_{(t,s) \in [0,\infty) \times [0,L]} \beta(\rho) > 0$  since by convergence of the flow,  $\rho(t, s)$  lies in a compact set for all  $(t, s)$ . By the assumptions on  $\omega$  and  $c_0$ , the function  $\kappa(t) - c_0$  has a zero in  $[0, L]$  for all  $t \geq 0$ . Therefore, (4.3) and Wirtinger's inequality imply

$$\frac{d}{dt} \mathcal{E}^\theta \leq \left( C \|\partial_t \rho\|_{L^\infty(0,L)} - \frac{4\pi^2}{L^2} \right) \int_0^L (\beta(\rho))^2 (\kappa - c_0)^2 ds,$$

where  $C = C(\beta, \theta, \rho) \in (0, \infty)$  is a constant independent of  $t \geq 0$ . Now,  $(\theta(t), \rho(t)) \rightarrow (\theta_\infty, \rho_\infty)$  in  $C^2([0, L])$  and (1.6) imply that  $\|\partial_t \rho\|_{L^\infty(0,L)} \rightarrow 0$  as  $t \rightarrow \infty$ . Consequently, we have

$$\frac{d}{dt} \mathcal{E}^\theta(t) \leq -\frac{4\pi^2 \inf_{(t,s)} \beta(\rho)}{2L^2} \mathcal{E}^\theta(t),$$

for  $t \geq T$  large enough, whence Gronwall's lemma yields  $\mathcal{E}^\theta(t) \leq Ce^{-\alpha t}$  for some appropriate  $C, \alpha > 0$ . It follows that  $\kappa = \partial_s \theta \rightarrow c_0$  in  $L^2(0, L)$  for  $t \rightarrow \infty$  exponentially fast. For the exponential convergence of  $\rho$ , we use (4.1) to conclude

$$\frac{d}{dt} \int_0^L (\rho - \nu)^2 ds \leq -2\mu \frac{4\pi^2}{L^2} \int_0^L (\rho - \nu)^2 ds + \sup_{(t,s)} |\nu - \rho| \frac{\sup_{(t,s)} |\beta'(\rho)|}{\inf_{(t,s)} \beta(\rho)} \mathcal{E}^\theta(t).$$

Using  $\mathcal{E}^\theta(t) \leq Ce^{-\alpha t}$ , the exponential convergence  $\rho \rightarrow \nu$  in  $L^2(0, L)$  follows with a Gronwall argument. Since  $\int_0^L \theta ds$  is preserved (cf. [10, Lemma 2.3]), we have  $\theta \rightarrow \phi + \frac{1}{L} \int_0^L \theta_0 ds - \pi$  as  $t \rightarrow \infty$  exponentially fast by the Poincaré–Wirtinger inequality. Theorem 1.1 and an interpolation argument imply that  $(\theta, \rho) \rightarrow (\phi + \frac{1}{L} \int_0^L \theta_0 ds - \pi, \nu)$  exponentially fast in  $C^{2+\tilde{\alpha}}([0, L])$  for all  $\tilde{\alpha} \in (0, \frac{1}{2})$ .  $\square$

Proposition 4.1 implies that if  $\omega = 1$  and  $c_0 = \frac{2\pi}{L}$ , there exists no nontrivial constrained critical point which is  $k$ -fold rotationally symmetric. Moreover, in this setting, Proposition 4.1 implies that for  $t$  large enough,  $\mathcal{E}^\theta(\theta, \rho)$  is eventually monotonically decreasing (compare to Section 3.1).

**4.2. Convergence to a homogeneous elastica for large  $\mu$ .** In Proposition 2.6, we have seen that for  $\omega \neq 0$  and large  $\mu$ , the  $\omega$ -fold covering of the circle with constant density is the unique global minimizer. In Theorem 1.6, we present a time-dependent version of this result if  $\rho_0 \equiv \nu$ . We point out that a constant initial density does not necessarily remain constant, see Remark 3.2, unless  $\beta'(\nu) = 0$  or  $\partial_s \theta_0 \equiv c_0$ .

*Proof of Theorem 1.6.* We assume that  $\int_0^L \theta_0(s) ds = \pi\omega L$ . This is no loss of generality because if  $(\theta, \rho)$  is the solution to (1.6) with initial datum  $(\theta_0, \rho_0) \in C^\infty([0, L])$ , then by a direct computation using trigonometric identities, it is readily checked that  $(\theta + r, \rho)$  is the solution to (1.6) with initial datum  $(\theta_0 + r, \rho)$  for  $r \in \mathbb{R}$ . Consider  $(\mu_j)_{j \in \mathbb{N}}$  such that  $\mu_j \rightarrow \infty$  for  $j \rightarrow \infty$ . By assumption,  $\mathcal{E}_{\mu_j}(\theta_0, \rho_0) =: K$  is independent of  $j \in \mathbb{N}$ . For any  $\mu_j$ , there exists a unique global solution  $(\theta_j, \rho_j)$  with initial datum  $(\theta_0, \rho_0)$  and this solution converges to some  $(\theta_{\infty,j}, \rho_{\infty,j}) \in C^\infty([0, L])$  in  $C^2([0, L])$  for  $t \rightarrow \infty$  (see Theorem 1.1 and Proposition 2.2). Since the integral of the angle is preserved (cf. [10, Lemma 2.3]), we have

$$(4.4) \quad \int_0^L \theta_{\infty,j}(s) ds = \int_0^L \theta_j(t, s) ds = \int_0^L \theta_0(s) ds = \pi\omega L \quad \text{for all } t \in (0, \infty), j \in \mathbb{N}.$$

Thus, we want to show that

$$(4.5) \quad (\theta_{\infty,j}, \rho_{\infty,j}) \rightarrow (\theta_c, \rho_c) \quad \text{in } C^1([0, L]) \quad \text{for } j \rightarrow \infty,$$

cf. Remark 2.5. Corollary 2.8 and (4.4) then allow us to conclude that for  $j$  large enough,  $(\theta_{\infty,j}, \rho_{\infty,j}) = (\theta_c, \rho_c)$  and the statement follows.

*Step 1: Uniform boundedness of  $\|(\theta_{\infty,j}, \rho_{\infty,j})\|_{W^{1,2}(0,L)}$ ,  $\lambda_{\theta 1}(\theta_{\infty,j}, \rho_{\infty,j})$ ,  $\lambda_{\theta 2}(\theta_{\infty,j}, \rho_{\infty,j})$ .* For this, we first observe that

$$(4.6) \quad \int_0^L (\partial_s \rho_{\infty,j})^2 \, ds \leq \frac{2}{\mu_j} K \rightarrow 0, \quad j \rightarrow \infty.$$

Since the integral of the density is fixed (see (1.5)), this yields  $\rho_{\infty,j} \rightarrow \nu$  in  $W^{1,2}(0,L)$  and in particular uniform boundedness of  $\|\rho_{\infty,j}\|_{W^{1,2}(0,L)}$  and  $\|\rho_{\infty,j}\|_{C([0,L])}$ . Thus, there is  $M \in \mathbb{R}$  (not depending on  $j$ ) such that

$$(4.7) \quad \int_0^L (\partial_s \theta_{\infty,j})^2 \, ds \leq \frac{K}{\inf_{[-M,M]} \beta} + 4\pi c_0 \omega.$$

With (4.4), we conclude that also  $\|\theta_{\infty,j}\|_{W^{1,2}(0,L)}$  is uniformly bounded. By [10, Lemma 4.1] and (4.7), the matrix  $\Pi^{-1}(\theta_{\infty,j})$  is bounded uniformly in  $j$ . Hence the bounds on  $\|\theta_{\infty,j}\|_{W^{1,2}(0,L)}$  and  $\|\rho_{\infty,j}\|_{C([0,L])}$  imply that

$$\begin{pmatrix} \lambda_{\theta 1} \\ \lambda_{\theta 2} \end{pmatrix} (\theta_{\infty,j}, \rho_{\infty,j}) = \Pi^{-1}(\theta_{\infty,j}) \int_0^L \begin{pmatrix} \cos \theta_{\infty,j} \\ \sin \theta_{\infty,j} \end{pmatrix} \partial_s \theta_{\infty,j} \beta(\rho_{\infty,j}) (\partial_s \theta_{\infty,j} - c_0) \, ds$$

is bounded uniformly in  $j \in \mathbb{N}$ .

*Step 2: Uniform boundedness of  $\|(\theta_{\infty,j}, \rho_{\infty,j})\|_{W^{2,2}(0,L)}$ .* To show boundedness of the  $L^2$ -norm of the second derivatives, we use that for all  $j \in \mathbb{N}$ ,  $(\theta_{\infty,j}, \rho_{\infty,j})$  is a stationary solution, i.e. a solution of (1.10). This allows to use similar arguments as in the proof of Proposition 2.2. First, we observe that

$$\|\partial_s (\beta(\rho_{\infty,j}) (\partial_s \theta_{\infty,j} - c_0))\|_{L^2(0,L)} = \|\lambda_{\theta 1} \sin \theta_{\infty,j} - \lambda_{\theta 2} \cos \theta_{\infty,j}\|_{L^2(0,L)}.$$

From Step 1, it follows that  $\beta(\rho_{\infty,j}) (\partial_s \theta_{\infty,j} - c_0)$  is bounded in  $W^{1,2}(0,L)$  uniformly in  $j \in \mathbb{N}$  and hence also in  $C([0,L])$ . By (1.9), this implies boundedness of  $\lambda_{\rho}(\theta_{\infty,j}, \rho_{\infty,j})$  and with that, (1.10) implies that  $\partial_s^2 \rho_{\infty,j}$  is uniformly bounded in  $L^2(0,L)$ . Now, we know that  $\rho_{\infty,j}$  is uniformly bounded in  $C^1([0,L])$  and since  $\beta(\rho_{\infty,j}) \geq \inf_{[-M,M]} \beta$ , this implies that  $\partial_s^2 \theta_{\infty,j}$  is uniformly bounded in  $L^2(0,L)$ . It follows that  $(\theta_{\infty,j}, \rho_{\infty,j})$  is bounded in  $W^{2,2}(0,L)$ , independently in  $j \in \mathbb{N}$ .

*Step 3:  $(\theta_{\infty,j}, \rho_{\infty,j}) \rightarrow (\theta_c, \rho_c)$  in  $C^1([0,L])$ .* Due to Step 2 and (4.6), there exists a (not relabeled) subsequence such that  $(\theta_{\infty,j}, \rho_{\infty,j}) \rightharpoonup (\theta_\infty, \nu)$  in  $W^{2,2}(0,L)$  and  $(\theta_{\infty,j}, \rho_{\infty,j}) \rightarrow (\theta_\infty, \nu)$  in  $C^1([0,L])$ . The limit  $(\theta_\infty, \nu)$  satisfies the Euler–Lagrange equations (2.2) and (2.3). Hence,  $(\theta_\infty, \nu)$  is a constrained critical point. With Proposition 2.2 it follows that  $\theta_\infty \in C^\infty([0,L])$ . Further, Lemma 2.9 implies that  $\theta_\infty$  describes an elastica. More precisely, (4.4) together with Remark 2.5 yields  $\theta_\infty = \frac{2\pi\omega}{L} s = \theta_c$ . Finally, a standard subsequence argument yields (4.5).  $\square$

## 5. NUMERICAL EXPERIMENTS

**5.1. Newton’s method for the gradient flow.** In the case  $\omega = 1$  and  $c_0 = 0$ , a numerical scheme to solve the static minimization problem (2.6) is proposed in [6]. We start by recalling the underlying idea and then explain how this can be extended to approximate solutions to (1.6).

*Numerical approximation of the static minimization problem.* The idea is to approximate the Euler–Lagrange equations (2.2)–(2.3) using finite differences, and to solve the resulting system with Newton’s method. We start by explaining the process formally: assuming that we have discretized space, we consider  $\hat{\eta} = (\hat{\theta}, \hat{\rho}) \in \mathbb{R}^{2N}$ , the piecewise constant approximation of  $\eta = (\theta, \rho)$ , as well as the corresponding energy  $\hat{\mathcal{E}}_\mu$ , along with  $\hat{\mathcal{E}}^\theta$ ,  $\hat{\mathcal{E}}_\mu^\rho$  and  $\hat{\mathcal{G}}$ . More generally, in what follows, a hat marks a space discrete quantity. We denote the set of admissible solutions by

$\{\hat{\eta} : \hat{\mathcal{G}}[\hat{\eta}] = 0 \in \mathbb{R}^d\}$ , where  $d$  is the number of constraints, so that the approximated minimization problem (2.6) can be written as

$$(5.1) \quad \min_{\hat{\mathcal{G}}[\hat{\eta}] = 0} \hat{\mathcal{E}}_\mu[\hat{\eta}].$$

The first order optimality conditions are given by

$$\begin{cases} \nabla \hat{\mathcal{E}}_\mu[\hat{\eta}] + D\hat{\mathcal{G}}[\hat{\eta}]^\top \Lambda = 0, \\ \hat{\mathcal{G}}[\hat{\eta}] = 0, \end{cases}$$

where  $\Lambda \in \mathbb{R}^d$  are the corresponding Lagrange multipliers. We can solve this system iteratively: assuming that the tuple  $(\hat{\eta}^j, \Lambda^j)$  is known, we linearize  $\hat{\mathcal{E}}_\mu$  and  $\hat{\mathcal{G}}$  around  $(\hat{\eta}^j, \Lambda^j)$  and get the following system, which is linear in  $(\hat{\eta}^{j+1} - \hat{\eta}^j, \Lambda^{j+1} - \Lambda^j)$ :

$$\begin{cases} \left( \nabla^2 \hat{\mathcal{E}}_\mu[\hat{\eta}^j] + \Lambda^j D^2 \hat{\mathcal{G}}[\hat{\eta}^j] \right) (\hat{\eta}^{j+1} - \hat{\eta}^j) \\ \quad + D\hat{\mathcal{G}}[\hat{\eta}^j]^\top (\Lambda^{j+1} - \Lambda^j) = -\nabla \hat{\mathcal{E}}_\mu[\hat{\eta}^j] - D\hat{\mathcal{G}}[\hat{\eta}^j]^\top \Lambda^j. \\ D\hat{\mathcal{G}}[\hat{\eta}^j] (\hat{\eta}^{j+1} - \hat{\eta}^j) = 0. \end{cases}$$

*Extension to the time-dependent problem.* Here, we use the same underlying idea and De Giorgi's minimizing movements to solve the corresponding  $L^2$ -gradient flow (1.6) numerically. To do this, we perform a time discretization with time step  $\tau$ , and consider the corresponding time discrete solution  $\hat{\eta}_\tau^n = \hat{\eta}_\tau(n\tau)$ , which is updated as follows:

$$\hat{\eta}_\tau^{n+1} \in \arg \min_{\hat{\mathcal{G}}(\hat{\eta}_\tau)=0} \frac{1}{2\tau} \|\hat{\eta}_\tau - \hat{\eta}_\tau^n\|_{L^2}^2 + \hat{\mathcal{E}}_\mu[\hat{\eta}_\tau].$$

This new minimization problem has the same structure as that of (5.1), so we can solve it with the method sketched above. For  $\tau$  and  $n$  given, this can be approximated as above, where the index  $n$  corresponds to the discretization in time and the index  $j$  to the discretization in space:

$$\begin{cases} \left( \frac{I_{2N}}{\tau} + \nabla^2 \hat{\mathcal{E}}_\mu[\hat{\eta}_\tau^{n+1,j}] + \Lambda_\tau^{n+1,j} D^2 \hat{\mathcal{G}}[\hat{\eta}_\tau^{n+1,j}] \right) (\hat{\eta}_\tau^{n+1,j+1} - \hat{\eta}_\tau^{n+1,j}) \\ \quad + D\hat{\mathcal{G}}[\hat{\eta}_\tau^{n+1,j}]^\top (\Lambda_\tau^{n+1,j+1} - \Lambda_\tau^{n+1,j}) = \\ \quad - \left( \frac{\hat{\eta}_\tau^{n+1,j} - \hat{\eta}_\tau^n}{\tau} + \nabla \hat{\mathcal{E}}_\mu[\hat{\eta}_\tau^{n+1,j}] + D\hat{\mathcal{G}}[\hat{\eta}_\tau^{n+1,j}]^\top \Lambda_\tau^{n+1,j} \right) \\ D\hat{\mathcal{G}}[\hat{\eta}_\tau^{n+1,j}] (\hat{\eta}_\tau^{n+1,j+1} - \hat{\eta}_\tau^{n+1,j}) = 0, \end{cases}$$

where  $I_{2N}$  is the identity matrix of size  $2N$ . This is a linear system with unknown  $(\hat{\eta}_\tau^{n+1,j+1} - \hat{\eta}_\tau^{n+1,j}, \Lambda_\tau^{n+1,j+1} - \Lambda_\tau^{n+1,j})$ . The inner loop (i.e. the loop in  $j$ ) is initialized by setting  $\hat{\eta}_\tau^{n+1,0} = \hat{\eta}_\tau^n$  and finalized with  $\hat{\eta}_\tau^{n+1} = \hat{\eta}_\tau^{n+1,j_\infty}$  (and similarly for  $\Lambda_\tau^{n+1}$ ). The iteration is stopped at  $j_\infty$ , corresponding to  $(\hat{\eta}_\tau^{n+1,j_\infty}, \Lambda_\tau^{n+1,j_\infty})$  fulfilling a convergence criterion, typically based on the  $L^2$ -norm of the residual, i.e. the right-hand side. This system has the form

$$(5.2) \quad \begin{aligned} & \begin{bmatrix} I_{2N} & 0 \\ 0 & 0 \end{bmatrix} + \tau \begin{bmatrix} \nabla^2 \hat{\mathcal{E}}_\mu[\hat{\eta}_\tau^{n+1,j}] + \Lambda_\tau^{n+1,j} D^2 \hat{\mathcal{G}}[\hat{\eta}_\tau^{n+1,j}] & D\hat{\mathcal{G}}[\hat{\eta}_\tau^{n+1,j}]^\top \\ D\hat{\mathcal{G}}[\hat{\eta}_\tau^{n+1,j}] & 0 \end{bmatrix} \begin{bmatrix} \hat{\eta}_\tau^{n+1,j+1} - \hat{\eta}_\tau^{n+1,j} \\ \Lambda_\tau^{n+1,j+1} - \Lambda_\tau^{n+1,j} \end{bmatrix} \\ & = - \begin{bmatrix} \hat{\eta}_\tau^{n+1,j} - \hat{\eta}_\tau^n \\ 0 \end{bmatrix} - \tau \begin{bmatrix} \nabla \hat{\mathcal{E}}_\mu[\hat{\eta}_\tau^{n+1,j}] + D\hat{\mathcal{G}}[\hat{\eta}_\tau^{n+1,j}]^\top \Lambda_\tau^{n+1,j} \\ 0 \end{bmatrix}. \end{aligned}$$

**5.2. Discretization.** As alluded to earlier, we consider a homogeneous discretization of  $[0, L]$  of size  $N$ , with  $s_i = iL/N = i\Delta s$  for  $0 \leq i < N$ . We can then define the space discrete functions  $\hat{\eta}_{\tau,i} = (\hat{\theta}_{\tau,i}, \hat{\rho}_{\tau,i}) = (\hat{\theta}_\tau(s_i), \hat{\rho}_\tau(s_i))$ . From the periodicity conditions, we extend the definition to  $-1 \leq i \leq N$  by defining  $\hat{\theta}_{\tau,-1} = \hat{\theta}_{\tau,N-1} - 2\omega\pi$ ,  $\hat{\theta}_{\tau,N} = \hat{\theta}_{\tau,0} + 2\omega\pi$ , as well as  $\hat{\rho}_{\tau,-1} = \hat{\rho}_{\tau,N-1}$ ,

$\hat{\rho}_{\tau,N} = \hat{\rho}_{\tau,0}$ . Because of the discontinuity in  $\theta$ , we also need to define the forward finite difference operator  $D_+ \hat{\theta}_\tau$  with

$$(D_+ \hat{\theta}_\tau)_i = \begin{cases} \hat{\theta}_{\tau,i+1} - \hat{\theta}_{\tau,i} & 0 \leq i < N-1 \\ \hat{\theta}_{\tau,0} + 2\pi\omega - \hat{\theta}_{\tau,N-1} & \text{otherwise.} \end{cases}$$

We define the backward (resp. centered) finite difference operator  $D_- \hat{\theta}_\tau$  (resp.  $D_c \hat{\theta}_\tau$ ) in the same fashion. The corresponding energy is  $\hat{\mathcal{E}}_\mu[\hat{\theta}_\tau, \hat{\rho}_\tau]$ :

$$\hat{\mathcal{E}}_\mu[\hat{\theta}_\tau, \hat{\rho}_\tau] = \frac{\Delta s}{2} \sum_{0 \leq i < N} \beta(\hat{\rho}_{\tau,i}) \left( \frac{(D_c \hat{\theta}_\tau)_i}{2\Delta s} - c_0 \right)^2 + \mu \left( \frac{\hat{\rho}_{\tau,i+1} - \hat{\rho}_{\tau,i}}{\Delta s} \right)^2,$$

and its gradient  $\nabla \hat{\mathcal{E}}_\mu = [\nabla_\theta \hat{\mathcal{E}}_\mu \ \nabla_\rho \hat{\mathcal{E}}_\mu]^T$  is approximated by:

$$\begin{aligned} (\nabla_\theta \hat{\mathcal{E}}_\mu[\hat{\theta}_\tau, \hat{\rho}_\tau])_i &= \Delta s \left[ \frac{\beta(\hat{\rho}_{\tau,i-1}) + \beta(\hat{\rho}_{\tau,i})}{2} \left( \frac{(D_- \hat{\theta}_\tau)_i}{\Delta s} - c_0 \right) - \frac{\beta(\hat{\rho}_{\tau,i}) + \beta(\hat{\rho}_{\tau,i+1})}{2} \left( \frac{(D_+ \hat{\theta}_\tau)_i}{\Delta s} - c_0 \right) \right] / \Delta s \\ (\nabla_\rho \hat{\mathcal{E}}_\mu[\hat{\theta}_\tau, \hat{\rho}_\tau])_i &= \Delta s \left[ \frac{\beta'(\hat{\rho}_{\tau,i})}{2} \left( \frac{(D_c \hat{\theta}_\tau)_i}{2\Delta s} - c_0 \right)^2 - \mu \frac{\hat{\rho}_{\tau,i-1} - 2\hat{\rho}_{\tau,i} + \hat{\rho}_{\tau,i+1}}{(\Delta s)^2} \right], \end{aligned}$$

where the expression for  $\nabla_\theta \hat{\mathcal{E}}_\mu$  is itself a finite difference, so that the divergence structure of the system is preserved at the discrete level. The constraints are written as:

$$\hat{\mathcal{G}}(\hat{\theta}_\tau, \hat{\rho}_\tau) = \Delta s \begin{bmatrix} \sum_{0 \leq i < N} \hat{\rho}_{\tau,i} - \nu L \\ \sum_{0 \leq i < N} \sin \hat{\theta}_{\tau,i} \\ \sum_{0 \leq i < N} \cos \hat{\theta}_{\tau,i} \end{bmatrix}, \quad \nabla \hat{\mathcal{G}}(\hat{\theta}_\tau, \hat{\rho}_\tau) = \Delta s \begin{bmatrix} \hat{\rho}_\tau & \cos \hat{\theta}_\tau & -\sin \hat{\theta}_\tau \end{bmatrix}.$$

For the sake of readability, we do not write the Hessian matrices of  $\hat{\mathcal{E}}_\mu$  and  $\hat{\mathcal{G}}$ .

**5.3. Stabilization of  $k$ -fold rotationally symmetric solutions.** As shown in Section 3.6.1, in the case  $\omega = 1$ ,  $k$ -fold rotational symmetry is preserved along the flow. For  $k > 1$ , such solutions are not numerically stable in general, and roundoff errors might lead to an incorrect asymptotic profile.

More precisely, let us define the real Fourier coefficients for  $u = \theta - \phi$  (which we identify with its periodic  $L$ -extension to  $\mathbb{R}$ ):

$$a_0^u = \frac{1}{L} \int_0^L u(s) \, ds, \quad a_i^u = \frac{2}{L} \int_0^L u(s) \cos \left( \frac{2\pi}{L} is \right) \, ds, \quad b_i^u = \frac{2}{L} \int_0^L u(s) \sin \left( \frac{2\pi}{L} is \right) \, ds,$$

where  $i \geq 1$ . The real Fourier coefficients  $a_0^\rho$ ,  $a_i^\rho$  and  $b_i^\rho$  are defined similarly.

A solution is  $k$ -fold rotationally symmetric if  $u$  and  $\rho$  are  $L/k$ -periodic, i.e. if

$$(5.3) \quad a_i^u = b_i^u = a_i^\rho = b_i^\rho = 0 \text{ if } i \geq 1 \text{ is not a multiple of } k.$$

In these terms, for the solution associated with  $k$ -fold rotationally symmetric initial datum, it can happen that the coefficient for some mode  $\ell < k$ , which is zero initially, becomes nonzero because of roundoff errors. If this mode is numerically unstable for the choice of parameters considered (esp.  $\mu$ ), this mode will grow and break the solution's symmetry.

To address this issue, we define the spaces which satisfy condition (5.3):

$$\tilde{V}_k := \left\{ \text{span} \left( (\cos(2\ell\pi s_i/L))_i, (\sin(2\ell\pi s_i/L))_i \right) : \exists q \in \mathbb{N} \text{ s.t. } \ell = qk \text{ and } \ell \leq \lfloor N/2 \rfloor \right\}^2,$$

$$V_k := \tilde{V}_k + \text{constants.}$$

Then, in the Newton iteration, instead of setting  $\hat{\eta}_\tau^{n+1} = \hat{\eta}_\tau^{n,j_\infty}$ , we set

$$\hat{\eta}_\tau^{n+1} = \hat{\eta}_{\tau,p}^{n,j_\infty} := \Pi_{\tilde{V}_k} \hat{\eta}_\tau^{n,j_\infty},$$

where the discrete  $L^2$ -orthogonal projection is done using the Fast Fourier Transform. Note that we exclude the space spanned by constants from the projection space, i.e. we do not project on  $V_k$  but on  $\tilde{V}_k$  (which does not contain constants), since the integrals of both  $\theta$  and  $\rho$  are preserved along the flow, so that the first Fourier coefficient of the increment  $\hat{\eta}_\tau^{n+1} - \hat{\eta}_\tau^n$  is always zero.

Description	Figure	$N$	$L$	$\mu$	$c_0$	$\beta(x)$	$\nu$	$\omega$	$k$
Loss of convexity	5	1440	$2\pi$	$10^{-1}$	1	$e^{-x}$	0	1	2
Loss of embeddedness for $c_0 > 2\pi/L$	6	720	$2\pi$	$10^{-3}$	3	$e^x$	0	1	2
Loss of embeddedness for $c_0 = 0$	7	1440	$2\pi$	1	0	$0.03 + bx^2$	$1/\pi$	1	2
$\hat{\mathcal{E}}_\mu(t)$ , $c_0 = 0$ , low $\ \hat{\kappa}_0 - 1\ _\infty$	8	720	$2\pi$	$10^{-3}$	0	$e^x$	0	1	5
$\hat{\mathcal{E}}_\mu(t)$ , $c_0 = 0$ , high $\ \hat{\kappa}_0 - 1\ _\infty$	9	720	$2\pi$	$10^{-3}$	0	$e^x$	0	1	5
$\hat{\theta}_0$ $\frac{L}{10}$ -periodic, $\hat{\rho}_0$ $\frac{L}{20}$ -periodic	10	720	$2\pi$	$10^{-3}$	0	$e^x$	0	1	10
$(\hat{\theta}_0, \hat{\rho}_0)$ as $\mu$ increases	11	420	$2\pi$	$10^{-2}$ to 5	0	$e^x$	0	2	-
$(\hat{\theta}_0, \hat{\rho}_0)$ as $\beta'$ decreases	11	420	$2\pi$	$10^{-2}$	0	$e^{ax}$	0	2	-
Figure eight	12	720	$2\pi$	$10^{-1}$	2	$0.1 + x^2$	0	0	-
2-fold figure eight	13	1440	$2\pi$	$10^{-1}$	0	$0.1 + x^2$	0	0	-

TABLE 1. Parameters used in the figures below. In the last column,  $k$  is given when the initial datum  $(\rho_0, c_0)$  is  $k$ -fold rotational symmetric.

**5.4. Results.** Here we give some example behavior of the solutions. First, in the case  $\omega = 1$ , we look at the possible loss of convexity and simplicity of the corresponding curve. Then, we give examples of the time evolution of the energies  $\hat{\mathcal{E}}$ ,  $\hat{\mathcal{E}}^\theta$  and  $\hat{\mathcal{E}}_\mu^\rho$  for small  $\mu$ , where we observe metastable energy plateaus. In this case, the bending energy  $\hat{\mathcal{E}}^\theta$  makes up most of the total energy  $\hat{\mathcal{E}}_\mu$ . Then, in the case  $\omega = 2$ , we illustrate how the choice of  $\beta$  and  $\mu$  can impact the limiting profile  $(\hat{\theta}_\infty, \hat{\rho}_\infty)$ . Finally, for  $\omega = 0$  and nonzero  $c_0$ , we look at the convergence of two curves, the first to the figure eight and the second to the 2-fold covering of the figure eight. All examples here correspond to  $L = 2\pi$ . A quick overview of the corresponding figures is given in Table 1.

**5.4.1. Loss of convexity.** In this section, we present a simple example illustrating the loss of convexity discussed in Example 3.7. As initial datum, we consider  $\hat{\theta}_0$  to be the discretization of a stadium of aspect ratio roughly equal to 1:5.  $\hat{\rho}_0$  is (the discretization of) a cosine function of amplitude 1. We take  $\beta : x \mapsto e^{-x}$ , and fix the parameters  $c_0 = 1$  and  $\mu = 10^{-1}$ . This situation is illustrated in Figure 5, where the loss of convexity is visible at time  $t \approx 0.05$ . We must note that, here, unlike in Example 3.7, the initial datum  $\hat{\rho}_0$  is not linear on the flat sides of the stadium.

By taking a very elongated stadium, it is reasonable to believe that the corresponding curve will not only lose convexity but also simplicity. In practice, it is difficult to show this behavior because of our choice of discretization, which enforces a homogeneous distribution of the nodes. An elongated stadium would require a very large  $N$  to resolve the rounded ends in a satisfying way. Instead, in the following, we choose a different initial condition, which also leads to loss of simplicity.

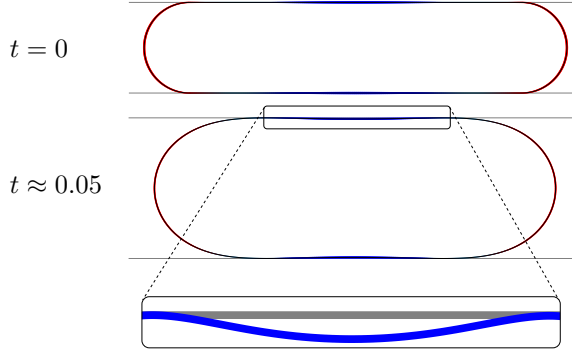


FIGURE 5. Loss of convexity of a stadium with sides parallel to the  $x$ -axis. Here and in subsequent figures, the width of the stroke increases with  $|\hat{\rho}|$ . For the sake of readability, the  $y$ -scale is amplified 10 times and the curve is shown with constant width in the inset. The gray lines are the tangents parallel to the  $x$ -axis, for reference. Here and in all the following figures, positive values of  $\rho$  are shown in blue, negative values in red. It is not shown here, but the curve becomes convex again at later times.

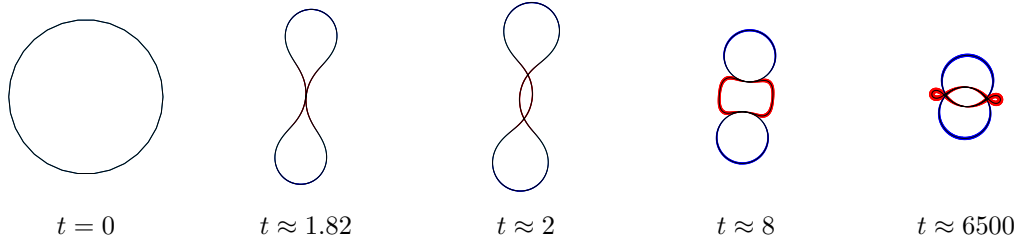


FIGURE 6. Snapshots of the solution showing the loss of embeddedness for  $c_0 = 3$ , starting from a convex initial datum.

5.4.2. *Simplicity (or embeddedness) along the flow.* In the case  $\omega = 1$ , we now investigate the possible loss of embeddedness of the curve along the evolution. We look at two different situations: first, starting with an initial datum corresponding to a convex curve, with  $c_0 > 2\pi/L$ . Second, for  $c_0 = 0$ , we carefully choose the initial datum such that  $\hat{\theta}_0$  corresponds to an embedded curve with a narrow neck. As the curve evolves, the sides of this neck come closer together and eventually cross.

*Loss of embeddedness, first case.* We start with  $c_0 = 3 > 2\pi/L$ ,  $\hat{\theta}_0$  close, but not equal, to  $\hat{\theta}_c$ , and  $\hat{\rho}_0$  corresponding to  $\cos(4\pi/Ls)$ , so that the initial datum is the discretization of a 2-fold rotationally symmetric curve. The solution at different times is drawn in Figure 6. The associated curve loses convexity and then embeddedness at  $t \approx 1.82$ , and the solution stays 2-fold rotationally symmetric, which is expected from the results of Section 3.6.1.

*Loss of embeddedness, second case.* In Proposition 3.11, the preservation of embeddedness of the curve described by  $\theta$  is proven for  $\omega = 1$ , provided the initial energy is small enough. Here, we provide a numerical example for which the discrete energy  $\hat{\mathcal{E}}_\mu(\hat{\theta}_0, \rho_0)$  is above the threshold given by Proposition 3.11, and for which embeddedness is lost along the flow.

To do so, we consider the choice of parameters  $\beta : x \mapsto 0.03 + bx^2$ ,  $b > 0$  and  $c_0 = 0$ . The energy threshold in Proposition 3.11 is then

$$\varepsilon := \frac{\inf \beta}{2} \left( \frac{C_{2T}}{L} - 4\pi c_0 + Lc_0^2 \right) \approx 0.35,$$

where we recall that we chose  $L = 2\pi$ , and that it holds  $C_{2T} \approx 146.628$ .

As initial datum, we pick a curve which can be described as consisting of two lateral drop-shaped lobes which are connected by a long, narrow neck. The initial datum  $\hat{\rho}_0$  is chosen positive and distributed in the concave parts of the lobes. Heuristically, the concave parts of the lobes concentrate a large part of the energy, and will quickly be “flattened” by the flow, making the two sides of the middle channel cross. We show numerically that this crossing does occur for  $b = 8$ .

A representation of the corresponding curve and initial distribution  $\hat{\rho}_0$  is shown in Figure 7A and 7B. For  $b = 8$ , we have  $\hat{\mathcal{E}}_\mu(\hat{\theta}_0, \hat{\rho}_0) \approx 16 > \varepsilon$ . Loss of embeddedness occurs at  $t_1 \approx 4.1 \times 10^{-3}$  with  $\hat{\mathcal{E}}_\mu(\hat{\theta}(t_1), \hat{\rho}(t_1)) \approx 10$ . The curve becomes simple again at  $t_2 \approx 2.91 \times 10^{-2}$  with  $\hat{\mathcal{E}}_\mu(\hat{\theta}(t_2), \hat{\rho}(t_2)) \approx 4.9 > \varepsilon$ . See Figure 7D. Note that at time  $t_2$  the energy is still one order of magnitude larger than the threshold given by Proposition 3.11. Simplicity is then kept for  $t > t_2$ .

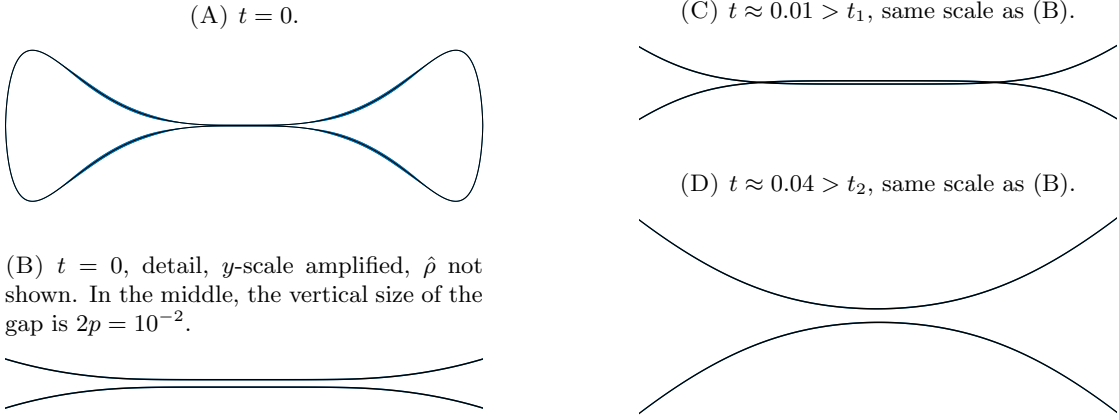


FIGURE 7. Snapshots showing that a simple curve does not need to stay simple along the flow, even for  $c_0 = 0$ . The choice of parameters is that of Section 5.4.2, here with  $b = 8$ .

5.4.3. *Evolution of the energy for  $\omega = 1$ , conservation of symmetry.* Here, we provide some examples of the time evolution of the different components of the energy, along with characteristic shapes of the solution as well as the associated density distribution  $\hat{\rho}$ . We are interested in cases where the solutions display a relatively rich behavior, so we choose  $\mu$  small, namely  $\mu = 10^{-3}$ . The bending stiffness  $\beta$  is chosen as  $\beta(x) = e^x$ , and we take zero total mass  $\nu L$ .

We consider two choices for the initial datum:

- The first with  $c_0 = 0$ , with low initial energy  $\hat{\mathcal{E}}_\mu$ , with  $\hat{\kappa}_0$  close to  $2\pi/L = 1$  and  $\hat{\rho}_0$  almost constant, see Figure 8.
- The second with  $c_0 = 0$ , with high initial energy, with  $\hat{\kappa}_0$  and  $\hat{\rho}_0$  oscillating significantly, see Figure 9.

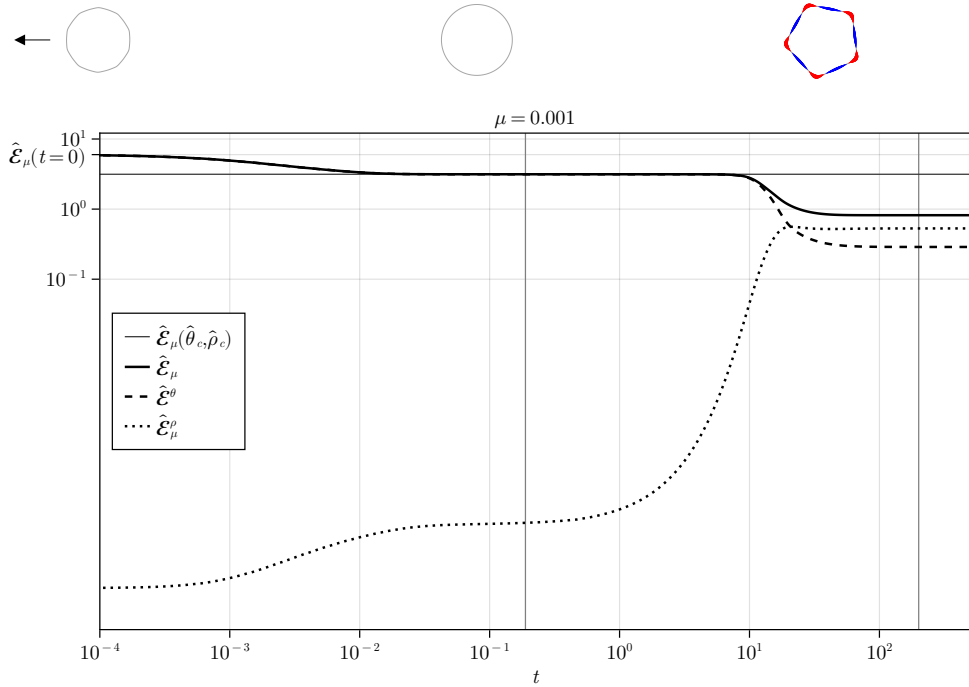


FIGURE 8. Energy evolution for  $c_0 = 0$ , starting with relatively low  $\|\hat{\kappa} - 1\|_\infty$  and 5-fold rotational symmetry.

In the two cases, both  $\hat{\theta}_0$  and  $\hat{\rho}_0$  are  $L/5$ -periodic, so that the initial datum is 5-fold rotationally symmetric, and the symmetry preserving results of Section 3.6.1 apply. In the second case,  $\hat{\theta}_0$  is not only  $L/5$ -periodic, but also  $L/10$ -periodic. The corresponding results are shown in Figure 8 and Figure 9, respectively. Because of the metastable nature of the evolution, both the time and the energy scales are logarithmic. Since  $\mu$  is small, with our choice of parameters, the main contribution to the initial energy  $\hat{\mathcal{E}}_\mu(\hat{\theta}_0, \hat{\rho}_0)$  comes from the bending energy  $\hat{\mathcal{E}}^\theta$ .

The shapes of the corresponding curves are naturally rather different: in the first case, the solution goes close to the trivial state  $(\hat{\theta}_c, \hat{\rho}_c)$  and spends some time there before changing to a pentagon-like curve, with positive values of  $\hat{\rho}$  on the flat “sides” and negative values on the rounded “corners”, which is in accordance with  $\nu L = 0$  and  $\beta$  monotone increasing.

In the second case, the solution does not come close to the trivial state, and the “dents” of the initial conditions coarsen, so that  $\hat{\theta}$  goes from being  $L/10$ -periodic to  $L/5$ -periodic. Eventually,  $(\hat{\theta}_\infty, \hat{\rho}_\infty)$  is identical to the first case, up to rotation.

This seems to suggests that, for this choice of parameters, the periodicity of the limiting profile is dictated by the choice of  $\hat{\rho}_0$ . However, one can take  $\hat{\rho}_0$  to be  $L/20$ -fold periodic by keeping all other parameters as in Figure 9, so that the initial datum is then 10-fold rotationally symmetric. The final profile is observed to be also  $L/10$ -symmetric, as shown in Figure 10, matching the periodicity of  $\hat{\theta}_0$  and not that of  $\hat{\rho}_0$ .

This shows numerically that for  $\mu$  small enough, there are  $k$ -fold rotationally symmetric critical points different from the homogeneous elastica, extending the picture drawn by Theorem 1.6.

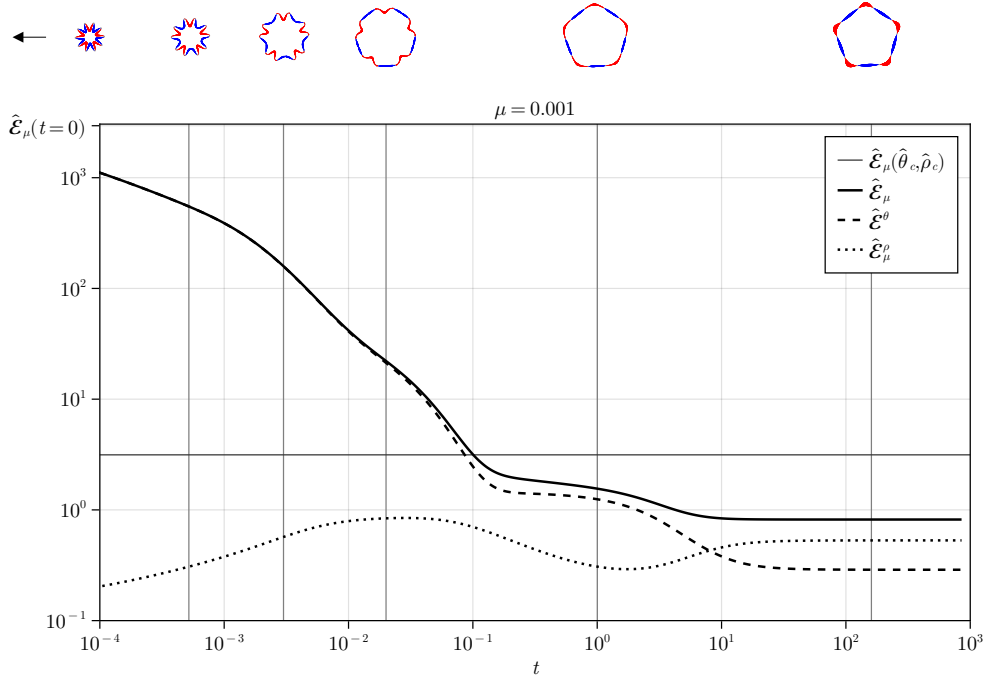


FIGURE 9. Energy evolution for  $c_0 = 0$ , starting with relatively large  $\|\hat{\kappa} - 1\|_\infty$  and 5-fold/10-fold rotational symmetry.

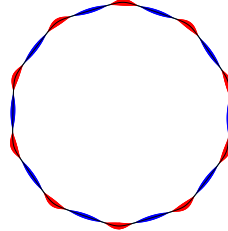


FIGURE 10. Representation of the  $L/10$ -periodic limiting profile of the solution with parameters identical to those of Figure 9, except that  $\hat{\rho}_0$  is  $L/20$ -periodic. As in Figure 9,  $\hat{\theta}_0$  is  $L/10$ -periodic.

5.4.4. *Influence of the model parameters for  $\omega = 2$ .* In Figure 11, starting from the same initial datum, we illustrate how the shapes assumed by the limit  $(\hat{\theta}_\infty, \hat{\rho}_\infty)$  change as the model parameters  $\mu$  and  $\beta$  change. The spontaneous curvature  $c_0$  is taken to be zero, and  $\beta$  is of the form  $\beta(x) = e^{ax}$ .

For relatively small values of  $\mu$  and large values of  $a$ , the solution is cigar- (or stadium-) shaped, with a small additional loop at one end, which accounts for  $\omega = 2$ , see Figure 11A and 11D. In those cases,  $\hat{\mathcal{E}}^\theta$  can be made small for a curve with flat sections corresponding to large values of  $\beta(\hat{\rho})$  (and highly curved sections corresponding to small values) without making  $\hat{\mathcal{E}}_\mu^\rho$  large thanks to the small value of  $\mu$ .

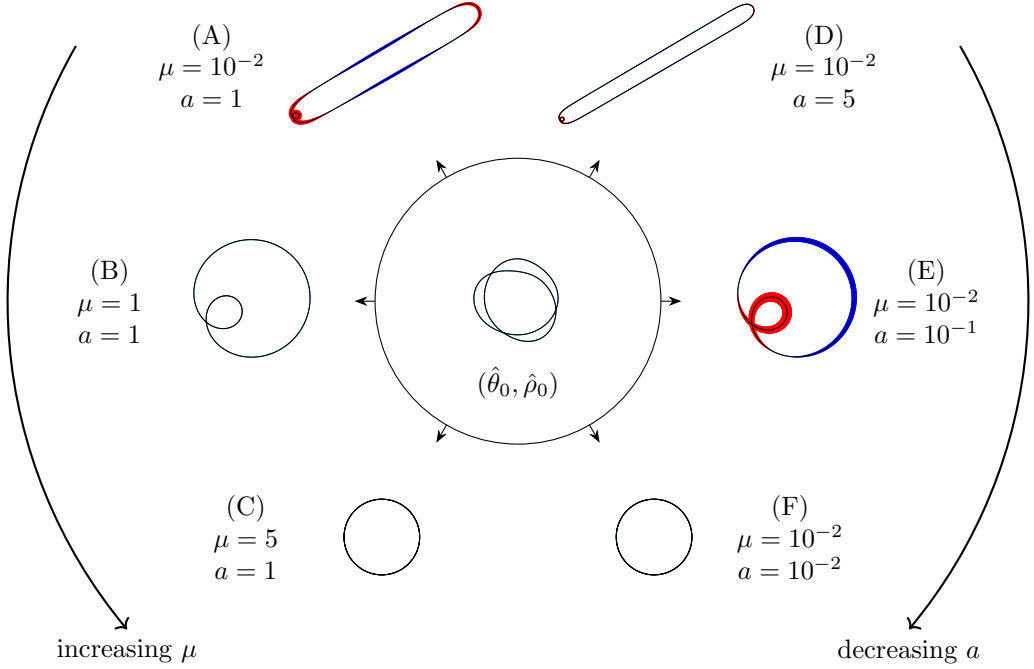


FIGURE 11. Illustration of the dependency of  $(\hat{\theta}_\infty, \hat{\rho}_\infty)$  on  $\mu$  and  $\beta$ . In both cases,  $\omega = 2$ ,  $c_0 = 0$  and  $\beta(x) = e^{ax}$ . Left:  $(\hat{\theta}_\infty, \hat{\rho}_\infty)$  as  $\mu$  increases in  $\{10^{-2}, 1, 5\}$  with  $a = 1$ . Right:  $(\hat{\theta}_\infty, \hat{\rho}_\infty)$  as  $a$  decreases in  $\{5, 10^{-1}, 10^{-2}\}$  with  $\mu = 10^{-2}$ . The initial datum is represented in the center.

As  $\mu$  increases, large values in the gradient of  $\hat{\rho}$  are penalized and the geometric part dominates, so that the curve becomes rounder as a result, cf. Figure 11B.

Increasing  $\mu$  further, in view of Theorem 1.6, it seems plausible that the solution should converge to  $(\hat{\theta}_c, \hat{\rho}_c)$ , although here the density  $\hat{\rho}_0$  is not constant. This is what can be observed in Figure 11C.

For what concerns  $a$ , i.e.  $\beta'$ , as it gets smaller (with  $\mu$  kept small), the gain in  $\hat{\mathcal{E}}^\theta$  coming from a given oscillation of density distribution diminishes, so the oscillation increases, see Figure 11E. Eventually, as  $a$  becomes very small, this is balanced by the increase in  $\hat{\mathcal{E}}_\mu^\rho$ , and the solution converges to the trivial state  $(\hat{\theta}_c, \hat{\rho}_c)$ , see Figure 11F.

5.4.5. *Convergence to the figure eight for  $\omega = 0$ .* To conclude this numerical overview, we look at the case  $\omega = 0$ , for which we recall that the only closed elasticae are multiple coverings of the figure eight, see Lemma 2.4.

More specifically, we consider two cases:

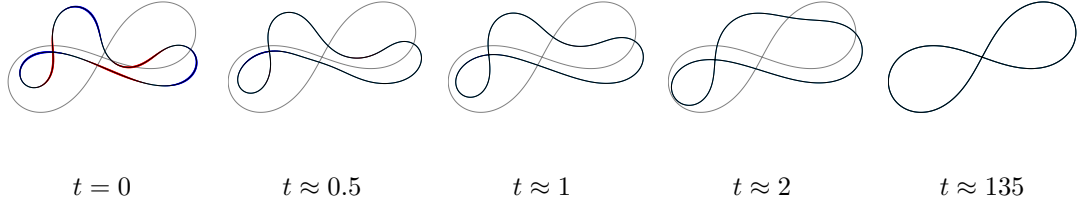


FIGURE 12. Convergence of an hand-drawn curve (black) to the figure eight (gray).  $\mu = 10^{-1}$ ,  $c_0 = 2$  and  $\beta(x) = 0.1 + x^2$  is quadratic and positive. We observe convergence to a homogeneous elastica. The figure eight in the background is the 1-fold covering of the figure eight whose integral of the corresponding tangential angle  $\theta$  matches that of the initial curve.

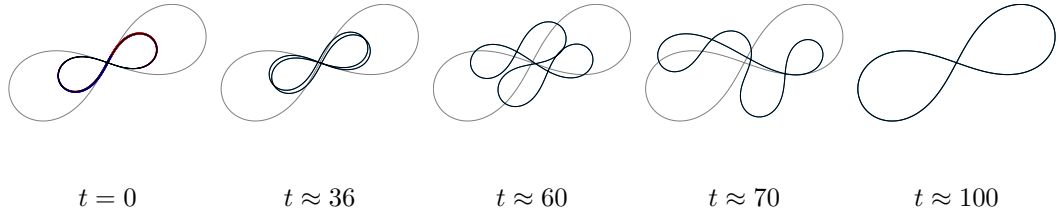


FIGURE 13. Evolution of the perturbation of a 2-fold covering of the figure eight, where the second is rotated by an angle of  $2\pi/1000$  with respect to the first one. Other parameters are  $\mu = 10^{-1}$ ,  $c_0 = 0$  and  $\beta(x) = 0.1 + x^2$ . The figure eight in the background is the 1-fold covering of the figure eight whose integral of the corresponding tangential angle  $\theta$  matches that of the initial curve.

- First,  $\hat{\theta}_0$  is given by a hand-drawn curve, with nonconstant  $\hat{\rho}_0$ . Here,  $c_0 = 2$ . See Figure 12.
- Second, in a very rough attempt to look at the stability of the 2-fold covering of the figure eight, we consider  $\hat{\theta}_0$  given by two slightly offset figure eights. We pick  $c_0 = 0$ . See Figure 13.

In both situations we take  $\nu = 0$  and  $\beta(x) = 0.1 + x^2$ , a choice which fits the assumptions of Theorem 1.5 with  $\bar{C} = 0$ , so that the limit is necessarily a (potentially multiple) covering of the figure eight. We observe convergence to the 1-fold covering of the homogeneous figure eight in both situations, which is expected in the first case. In the second case, this suggests that the multiple coverings of the figure eight are not stable under the flow, at least for this choice of  $\beta$ .

#### REFERENCES

- [1] H. Abels, F. Bürger, and H. Garcke. Qualitative properties for a system coupling scaled mean curvature flow and diffusion. *J. Differential Equations*, 349:236–268, 2023.
- [2] H. Abels, F. Bürger, and H. Garcke. Short time existence for coupling of scaled mean curvature flow and diffusion. *J. Evol. Equ.*, 23(1):Paper No. 14, 46, 2023.
- [3] S. B. Angenent. The zero set of a solution of a parabolic equation. *Journal für die reine und angewandte Mathematik (Crelles Journal)*, 1988:79 – 96, 1988.
- [4] T. Baumgart, S. T. Hess, and W. W. Webb. Imaging coexisting fluid domains in biomembrane models coupling curvature and line tension. *Nature*, 425:821–824, 2003.

- [5] S. Blatt. Loss of convexity and embeddedness for geometric evolution equations of higher order. *J. Evol. Equ.*, 10(1):21–27, 2010.
- [6] K. Brazda, G. Jankowiak, C. Schmeiser, and U. Stefanelli. Bifurcation of elastic curves with modulated stiffness. *European Journal of Applied Mathematics*, page 1–27, 2022.
- [7] K. Brazda, L. Lussardi, and U. Stefanelli. Existence of varifold minimizers for the multiphase Canham-Helfrich functional. *Calc. Var. Partial Differential Equations*, 59(3):Paper No. 93, 26, 2020.
- [8] P. Canham. The minimum energy of bending as a possible explanation of the biconcave shape of the human red blood cell. *J. Theor. Biol.*, 26(1):61–81, 1970.
- [9] R. Choksi, M. Morandotti, and M. Veneroni. Global minimizers for axisymmetric multiphase membranes. *ESAIM Control Optim. Calc. Var.*, 19(4):1014–1029, 2013.
- [10] A. Dall'Acqua, L. Langer, and F. Rupp. A dynamic approach to heterogeneous elastic wires. *arXiv*, 2205.06587, 2022.
- [11] A. Dall'Acqua, C.-C. Lin, and P. Pozzi. A gradient flow for open elastic curves with fixed length and clamped ends. *Ann. Sc. Norm. Super. Pisa Cl. Sci. (5)*, 17(3):1031–1066, 2017.
- [12] A. Dall'Acqua and P. Pozzi. A Willmore-Helfrich  $L^2$ -flow of curves with natural boundary conditions. *Comm. Anal. Geom.*, 22(4):617–669, 2014.
- [13] A. Dall'Acqua, P. Pozzi, and A. Spener. The Lojasiewicz-Simon gradient inequality for open elastic curves. *J. Differential Equations*, 261(3):2168–2209, 2016.
- [14] P. A. Djondjorov, M. T. Hadzhilazova, I. M. Mladenov, and V. M. Vassilev. Explicit parameterization of Euler's elastica. *Geometry, integrability and quantization*, pages 175 – 186, 2008.
- [15] P. Dondl, C. A. Hounkpe, and M. Jesenko.  $\Gamma$ -convergence of a discrete Kirchhoff rod energy. *arXiv*, 2306.10936, 2023.
- [16] G. Dziuk, E. Kuwert, and R. Schätzle. Evolution of elastic curves in  $\mathbb{R}^n$ : existence and computation. *SIAM J. Math. Anal.*, 33(5):1228–1245, 2002.
- [17] C. M. Elliott, H. Garcke, and B. Kovács. Numerical analysis for the interaction of mean curvature flow and diffusion on closed surfaces. *Numerische Mathematik*, 151(4):873–925, Aug. 2022.
- [18] J. Escher and K. Ito. Some dynamic properties of volume preserving curvature driven flows. *Math. Ann.*, 333(1):213–230, 2005.
- [19] M. Gage and R. S. Hamilton. The heat equation shrinking convex plane curves. *J. Differential Geom.*, 23(1):69–96, 1986.
- [20] W. Helfrich. Elastic properties of lipid bilayers: Theory and possible experiments. *Zeitschrift für Naturforschung C*, 28(11):693–703, 1973.
- [21] M. Helmers. Snapping elastic curves as a one-dimensional analogue of two-component lipid bilayers. *Math. Models Methods Appl. Sci.*, 21(5):1027–1042, 2011.
- [22] M. Helmers. Convergence of an approximation for rotationally symmetric two-phase lipid bilayer membranes. *Q. J. Math.*, 66(1):143–170, 2015.
- [23] F. Jülicher and R. Lipowsky. Domain-induced budding of vesicles. *Phys. Rev. Lett.*, 70:2964–2967, May 1993.
- [24] J. Langer and D. A. Singer. The total squared curvature of closed curves. *Journal of Differential Geometry*, 20(1):1 – 22, 1984.
- [25] C.-C. Lin.  $L^2$ -flow of elastic curves with clamped boundary conditions. *J. Differential Equations*, 252(12):6414–6428, 2012.
- [26] C.-C. Lin, Y.-K. Lue, and H. R. Schwetlick. The second-order  $L^2$ -flow of inextensible elastic curves with hinged ends in the plane. *J. Elasticity*, 119(1-2):263–291, 2015.
- [27] A. Linnér. Some properties of the curve straightening flow in the plane. *Trans. Amer. Math. Soc.*, 314(2):605–618, 1989.
- [28] A. Linnér. Unified representations of nonlinear splines. *J. Approx. Theory*, 84(3):315–350, 1996.
- [29] C. Mantegazza, A. Pluda, and M. Pozzetta. A survey of the elastic flow of curves and networks. *Milan J. Math.*, 89(1):59–121, 2021.
- [30] C. Mantegazza and M. Pozzetta. The Lojasiewicz-Simon inequality for the elastic flow. *Calc. Var. Partial Differential Equations*, 60(1):Paper No. 56, 17, 2021.
- [31] H. T. McMahon and J. L. Gallop. Membrane curvature and mechanisms of dynamic cell membrane remodelling. *Nature*, 438:590–596, 2005.
- [32] T. Miura, M. Müller, and F. Rupp. Optimal thresholds for preserving embeddedness of elastic flows. *To appear in Amer. J. Math.*, arXiv:2106.09549, 2021.
- [33] M. Müller and F. Rupp. A Li-Yau inequality for the 1-dimensional Willmore energy. *Adv. Calc. Var.*, 16(2):337–362, 2023.
- [34] M. Müller and A. Spener. On the convergence of the elastic flow in the hyperbolic plane. *Geom. Flows*, 5(1):40–77, 2020.

- [35] M. Novaga and P. Pozzi. A second order gradient flow of  $p$ -elastic planar networks. *SIAM J. Math. Anal.*, 52(1):682–708, 2020.
- [36] S. Okabe, P. Pozzi, and G. Wheeler. A gradient flow for the  $p$ -elastic energy defined on closed planar curves. *Math. Ann.*, 378(1-2):777–828, 2020.
- [37] F. Rupp. On the Łojasiewicz-Simon gradient inequality on submanifolds. *J. Funct. Anal.*, 279(8):108708, 33, 2020.
- [38] Y. Wen.  $L^2$  flow of curve straightening in the plane. *Duke Mathematical Journal*, 70(3):683 – 698, 1993.
- [39] E. Zeidler. *Nonlinear Functional Analysis and its Applications - III: Variational Methods and Optimization*. Translated by L. F. Boron. Springer-Verlag, New York, 1985.

(A. Dall'Acqua) INSTITUTE OF APPLIED ANALYSIS, ULM UNIVERSITY, HELMHOLTZSTRASSE 18, 89081 ULM, GERMANY.

*Email address:* anna.dallacqua@uni-ulm.de

(G. Jankowiak) DEPARTMENT OF MATHEMATICS AND STATISTICS, UNIVERSITY OF KONSTANZ, 78457 KONSTANZ, GERMANY.

*Email address:* gaspard.jankowiak@uni-konstanz.de

(L. Langer) INSTITUTE OF APPLIED ANALYSIS, ULM UNIVERSITY, HELMHOLTZSTRASSE 18, 89081 ULM, GERMANY.

*Email address:* leonie.langer@uni-ulm.de

(F. Rupp) FACULTY OF MATHEMATICS, UNIVERSITY OF VIENNA, OSKAR-MORGENSTERN-PLATZ 1, 1090 VIENNA, AUSTRIA.

*Email address:* fabian.rupp@univie.ac.at